IEEE Access
Multidisciplinary | Rapid Review | Open Access Journal

Received November 4, 2016, accepted November 28, 2011, date of publication December 28, 2016, date of current version March 2, 2017.

Digital Object Identifier 10.1109/ACCESS.2016.2644607

Optimal Power Control in Green Wireless Sensor Networks With Wireless Energy Harvesting, Wake-Up Radio and Transmission Control

CHINMAYA MAHAPATRA[1], ZHENGGUO SHENG[2], POUYA KAMALINEJAD[1], VICTOR C.M. LEUNG[1], AND SHAHRIAR MIRABBASI[1]

[1]Department of Electrical and Computer Engineering, University of British Columbia, Vancouver, BC V6T 1Z4, Canada
[2]Department of Engineering and Design, University of Sussex, Brighton BN1 9RH, U.K.

Corresponding author: C. Mahapatra (chinmaya@ece.ubc.ca)

This work was supported in part by the Natural Sciences and Engineering Research Council of Canada, in part by the ICICS People and Planet Friendly Home Initiative at University of British Columbia, in part by TELUS, and in part by other industry partners.

ABSTRACT Wireless sensor networks (WSNs) are autonomous networks of spatially distributed sensor nodes that are capable of wirelessly communicating with each other in a multihop fashion. Among different metrics, network lifetime and utility, and energy consumption in terms of carbon footprint are key parameters that determine the performance of such a network and entail a sophisticated design at different abstraction levels. In this paper, wireless energy harvesting (WEH), wake-up radio (WUR) scheme, and error control coding (ECC) are investigated as enabling solutions to enhance the performance of WSNs while reducing its carbon footprint. Specifically, a utility-lifetime maximization problem incorporating WEH, WUR, and ECC, is formulated and solved using distributed dual subgradient algorithm based on the Lagrange multiplier method. Discussion and verification through simulation results show how the proposed solutions improve network utility, prolong the lifetime, and pave the way for a greener WSN by reducing its carbon footprint.

INDEX TERMS Green wireless sensor network (GWSN), wireless energy harvesting (WEH), wake-up radio (WUR), error control coding (ECC), subgradient algorithm.

I. INTRODUCTION

Wireless Sensor Networks (WSNs) is a smart and intelligent infrastructure of uniquely identifiable devices capable of wirelessly communicating with each other through the Internet. Its technologies are used to monitor many aspects of a city in real time. For example, the networked heterogeneous devices connected in a smart structure are typically equipped with sensors, sink nodes, wireless transceivers, cloud servers and finite battery supply to monitor and send/receive data. With the development of Internet-of-Things (IoT), a wide range of intelligent and tiny wireless sensing devices have been massively deployed in a variety of application environments such as home automation, healthcare, surveillance, transportation, smart environments and many more.

Although the WSN systems possess tremendous potential but there are many dominant barriers in implementing such a grandiose scheme. For example, the limited battery capacity, on-chip memory and small transmit power, the lifetime of sensor devices, its processing capability and range of operation are curtailed [1]. Moreover, the sensor devices that are farther from sink nodes or that work as relay node are drained quickly of their battery and may negatively affect the overall system performance. The Information and Communication Technologies (ICT) is currently responsible for 2 to 4 % of the current total carbon emissions or footprint [2]. In the future, as the plethora of smart devices connected to each other utilizing WSNs will be deployed, the carbon footprint is going to increase manyfold and will be responsible for a larger percentage of carbon emissions [2]. The current systems are not equipped to deal with this issue. Hence, it is necessary to analyze the system lifetime by minimizing its total energy consumption and carbon footprint without degrading the desired application performance and reliability constraints. Motivated by the emerging concept of Green Wireless Sensor Network (GWSN) in which the lifetime and throughput performance of the system is maximized while minimizing the carbon footprints, our goal is to build an sustainable WSN system by supplying adequate energy to

2169-3536 © 2016 IEEE. Translations and content mining are permitted for academic research only.
Personal use is also permitted, but republication/redistribution requires IEEE permission.
See http://www.ieee.org/publications_standards/publications/rights/index.html for more information.

improve the system lifetime and providing reliable/robust transmission without compromising overall quality of service.

II. PRIOR RELATED WORKS, MOTIVATION AND CONTRIBUTION

Optimization methods have been extensively used in previous research works to solve for network lifetime of wireless sensor networks. Network lifetime maximization with flow rate constraint have been studied in many prior works. Kelly *et al.* was the first to propose two classes of distributed rate control algorithms for communication networks [3]. Madan and Lall [4] solved the lifetime maximization problem with a distributed algorithm using the subgradient method. Ehsan *et al*. [5] propose an energy and cross-layer aware routing schemes for multichannel access WSNs that account for radio, MAC contention, and network constraints, to maximize the network lifetime. But, the problems formulated and solved in all these approaches neither does take into account a proper energy model incorporating all the transceiver resources nor it involves the application performance trade-off due to increase in lifetime by decreasing rate flows.

System utility and network lifetime are problems that are related to each other in a reciprocal relationship meaning maximizing one will degrade the other. Chen *et al*. [6] analyzed the utility-lifetime trade-off in wireless sensor network for flow constraints. He *et al*. [7] followed a cross-layer design approach. Both of these papers take transmission rate as the sole indicator of the system throughput, which is not true as the reliability plays a vital role in determining the system performance. Reliability in the system can be improved by introducing error control schemes into the sensor nodes with multipath routing introduced by lun *et al*. [8]. Yu *et al*. [9] analyses the automatic repeat request (ARQ) as well as a hybrid ARQ scheme for WSNs. The ARQ scheme requires re-transmission if there is a failure of packet delivery which increases energy consumption of node. Xu *et al*. [10] describes a rate-reliability and lifetime trade-off for WSNs by taking theoritical end to end error probability of packets. Similarly, Zou *et al*. [11] has taken a joint lifetime-utility-rate-reliability approach for WSNs taking a generic error coding processing power model. Both [10] and [11] lack the inclusion and analysis of an error control scheme with their encoding/decoding powers as well as the delay performance of the overall system with error correction employed.

Energy harvesting is proposed as a possible method to improve the network lifetime and rechargeable batteries in WSNs by He *et al*. [12], Magno *et al*. [13], Deng *et al*. [14] and Kamalinejad *et al*. [15]. Practically, energy can be harvested from the environmental sources, namely, thermal, solar, vibration, and wireless radio-frequency (RF) energy sources [16]. While harvesting from the aforementioned environmental sources is dependent on the presence of the corresponding energy source, RF energy harvesting provides key benefits in terms of being wireless, readily available in the form of transmitted energy (TV/radio broadcasters, mobile base stations and hand-held radios), low cost, and small form factor implementation. Recently, dynamics of traffic and energy replenishment incorporated in the network power model has been an active research topic. Some of the challenges are addressed by [17], [18], and [19]. They assume battery energy to be zero at start, which may not be practical for many application scenarios that has sensors with rechargeable batteries. challenges caused by packet loss due to interference has also not been addressed.

Green networking of late in the past four to five years has attracted a lot of attention. Koutitas [20] has analyzed a maximization problem based on carbon footprints generated in terrestrial broadcasting networks. Naeem *et al*. [21] have maximized the data rate while minimizing the CO_2 emissions in cognitive sensor networks. But it is yet to be seen how much carbon emissions can be minimized while maximizing the utility and lifetime with reliability and energy harvesting constraints.

In this paper, we formulate and solve a joint maximization problem of system performance (measured by data utilization) and lifetime for wireless sensor network. The packet loss and data utilizations are incorporated to provide a more realistic data loss and utilization model for the WSN system. As energy is scarce resource for a WSN system, energy harvesting is adapted in the system model to increase its lifetime. We model the harvesting as a stochastically varying. Contrary to articles [17], [18], and [19], our model assumes that the battery starts with a initial energy and the network operations has to be sustained using harvesting and wake up radio (WUR), using harvesting from ambient RF energy rather than using a solar energy harvester which needs extra circuitry. The overall problem throws challenges in finding an optimal solution as the time-variation combined with retransmissions, packet loss and harvesting makes it complex. We, then provide a distributed solution to the problem by solving the data-utility and network lifetime separately. Our major contributions are summarized as follows:

(1) We formulate the data-utility lifetime trade-off problem by taking an approximated lifetime function as well as the energy harversting, wake up radio duty cycling and retransmissions into the utility function.

(2) We propose a redundant residue number system based error correcting technique and compare it with ARQ and Bose-Chaudhuri-Hocquenghem (BCH). Innovatively, the packet error rate and delay are being included while computing lifetime and performance of the sensor network.

(3) We show how the energy harvesting and error control coding can jointly reduce carbon footprints generated per year and make the network green.

As per the best knowledge of the author, this is the first paper that incorporates wireless energy harvesting and error control coding into the power model of the objective function. The rest of this paper is organized as follows. Section II presents the prior works. System model formulation is

described in Section III. Section IV describes our error control coding based data transmission control. In Section V, we propose the WEH and WUR schemes for WSN system. In Section VI, we formulate the joint utility-lifetime trade-off problem and formulate a distributed solution based on subgradient method. Section VII shows our simulation plots followed by conclusion in Section VIII.

III. SYSTEM MODEL AND PROBLEM FORMULATION

We consider a network with static and identical sensor nodes denoted by N. Sensor nodes collect data from the surrounding information field and deliver it to the sink node/collector node denoted by S. As in [22], sensors communicate either in an uniformly distributed ring topology or randomly in a multi-hop ad-hoc topology. We assume that the sensor devices in an WSN system are transmitting over a set of links L. We model the wireless network as a {node, link} connectivity graph $G(Z, L)$, where the set, $Z = N \cup S$, represents the source and sink nodes. The set of links, L, represents the communication link between the nodes. Two nodes i and j are connected if they can transmit packets to each other with $i \in N$ and $j \in N_i$, where N_i is the number of outgoing sensor nodes from source to sink. Fig. 1 shows a sample connectivity graph with three sensor nodes ($i1, i2, i3$), one sink node ($s1$) and six communication links ($l1, l2, l3, l4, l5, l6$). The communication between node $i1$ and $s1$ is a single-hop transmission whereas between $i3$ and $s1$ denotes a multi-hop transmission with node $i2$ acting as relay for data of node $i3$. The set of outgoing links and the set of incoming links corresponding to a node i are denoted by $O(i)$ and $I(i)$ respectively. Thus, in Fig. 1, $O(i2) = (l3, l6)$ and $I(i2) = (l4, l5)$. Table 1 delineates the parameters used for the analysis of our scenarios.

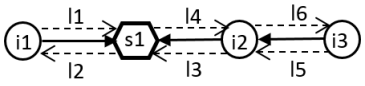

FIGURE 1. Connectivity graph.

A. ROUTING AND FLOW CONSERVATION

We model the data transmission rates and routing of data in the network using flow conservation equation. Let r_{ij} denote the rate of information flow from nodes i to node j. Let R_{ij} denote the total information rate generated at source node i to be communicated to sink node $j \in N_i$. It is assumed that no compression is performed at the source node. Thus satisfying flow conservation constraint, we have the flow equations at the nodes for time slot t as

$$\sum_{j \in N_i} \big(r_{ij}(t) - r_{ji}(t)\big) = R_{ij}(t), \forall i \in N, j \in N_i \qquad (1)$$

The maximum transmission rate of a link is also known as its capacity C_l. For a given transmit power of node and bandwidth of the channel, this value is fixed and is a upper bound of r_{ij} as $0 \leq r_{ij} \leq C_l$.

TABLE 1. Notations used in the paper.

Symbol	Description
$\|.\|_\infty$	∞-norm
$\|.\|_p$	p-norm
N	Set of Sensor Nodes
S	Set of Sink Nodes
i	Outgoing Sensor Node
j	Incoming Sensor Node
r_{ij}	Rate of Information Flow between i & j
R_{ij}	Source rate
C_l	Capacity of Link
$T_{network}$	Lifetime of Network
E_{TX}	Transmit energy [J/bit]
E_{RX}	Receive energy [J/bit]
E_{PR}	Processing energy [J/bit]
E_{SN}	Sensing energy [J/bit]
P_{LS}	Listening power [W]
E_B	Battery energy of Sensor
P_H	Harvested power
$W_U^{'}$	Wake-up-radio on-off signal
γ	Path loss exponent
d	Communication distance
P_e	Packet Loss Rate
P_s	Packet Success Rate
P_b	Bit error rate
L_P	Length of packet
$E(T)$	Expected number of retransmissions
h	Number of hops
$GF(2^b)$	Galois Field of b-bits
$U(.)$	Utility function
α	System design parameter
ϵ	Lifetime approximation constant
F_{CO_2}	Total Carbon footprint

B. ENERGY COST MODEL

The network lifetime is dependent on the power consumption of the sensor node P_i per active duty cycle slot T_i of a node. This involves the combined operations of sensing, processing and communication (receive/transmit). If a sensor node goes out of the service due to energy deficiency, then all the sensing services from that node are affected till the battery is replaced.

Radio transceiver is the one of the most power hungry block of a sensor device. The communication energy per bit per time slot $E_{comm}(t)$ consists of $E_{RX}(t)$ (receiver energy per bit per time slot) and $E_{TX}(t)$ (transmitter energy per bit per time slot). The computation energy includes $E_{PR}(t)$

(processing energy per bit per slot) and $E_{SN}(t)$ (sensing energy per bit per time slot). Let, $E_B(t) \geq 0$ is the total residual energy left in a sensor node operated by battery at time slot t. The power consumption in a time slot t is modeled as

$$P_i(t) = \sum_{i\in N, j\in N_i} r_{ij}(t)E_{TX}(t) + \sum_{i\in N, j\in N_i} r_{ji}(t)E_{RX}(t) + \sum_{i\in N, j\in N_i} R_{ij}(t)E_{PR}(t) + \sum_{i\in N, j\in N_i} R_{ij}(t)E_{SN}(t) \quad (2)$$

From the communication energy model in [4], we modify our transmitter energy for transmitting one bit of data from $i\in N$ to $j\in N_i$ across distance d as

$$E_{TX} = a_1 + a_2 \cdot d_{ij}^{\gamma} \quad (3)$$

Where γ is the path loss exponent varying from $\gamma\in[2, 6]$, a_1 and a_2 are constants depending on the characteristics of the transceiver circuit.

IV. PACKET LOSS AND DATA RE-TRANSMISSION

A fundamental approach to reduce the packet loss is necessary to be integrated together with upper layer protocols to deliver reliable WSN management in an interfering environment. As often as the packets are failed to be delivered to the sink node, the re-transmission consumes extra energy from the battery source of the sensor node, thereby decreasing its lifetime substantially. We assume a TDMA based MAC protocol where retransmission occurs till time-out after which the packet is dropped. The packet loss is dependent on the data traffic. We propose to use the approach of Error Correction Coding (ECC) to improve transmission reliability. ECC adds redundancy to improve the transmission reliability thereby reducing the efficiency, it is still a more preferable solution, because it helps to improve both reliability and latency. In this paper, we describe a error coding scheme on the theoretical basis of Redundant residue number systems (RRNS). An analysis of the our proposed RRNS has been done in [23] that has been extended into our system model in this paper. We have briefly explained the coding scheme and its merits as compared to other lightweight coding schemes. Schemes such as Turbo-codes or viterbi codes need heavy resources for their implementation. So, they are not considered for this analysis in WSN. Reader is referred to our paper [23] for a detailed description.

Our main goal in this section is to introduce the current transmission scheme ARQ and give a brief description why ECC based schemes are advantageous. From ECC schemes of BCH and RRNS [23], our scheme provides improved performance and is thus incorporated for analysis in the optimization problem.

1) ANALYSIS OF PACKET ERROR IN ARQ SCHEME

In ARQ scheme, data is decoded by cyclic redundancy check (CRC) codes and the erroneous data is re-transmitted from the sender. Here we consider stop and wait ARQ method. Assuming the ACK bits are received without error, the packet error rate of the ARQ scheme is given by

$$P_e^{ARQ} = 1 - (1 - P_b)^{L_P} \quad (4)$$

where L_P is the packet length of the payload transmitted in a single transmission, P_b is the bit error rate. P_b for sensor nodes in IEEE 802.15.4 is given in [24].

2) ANALYSIS OF PACKET ERROR IN ECC SCHEMES

Let us assume that we use a (n, k, e) e-error control method with $n - k$ redundant bits appended to the k-data bits. We further assume that the transmission of the packets between the sensor node and sink node is in bursts of n-bit data. Therefore, the packet loss rate at the sink node is given as

$$P_e^{ECC} = 1 - \left(1 - \sum_{i=e+1}^{n} \binom{n}{i} P_b^i (1 - P_b)^{n-i}\right)^{\left\lceil \frac{L_P}{k} \right\rceil} \quad (5)$$

Where $\lceil . \rceil$ is the ceiling function. We assume that due to poor channel conditions and interference, when a packet is unsuccessful in reaching its destination, it is counted as loss of packet and a re-transmission is required. The packet is assumed to be successfully delivered when the acknowledgement (ACK) for the delivery is received. Thus it takes one complete trip for the packet to be assured as successfully delivered.

Lemma 1: Let P_e be the probability of an event where the packet is lost in being delivered from sensor to sink or the ACK failed to reach the sensor from sink. Thus, for a single hop the expected number of re-transmissions is given by

$$E(Tr) = \frac{1}{(1 - P_e)} \quad (6)$$

Where, P_e is the packet loss rate of ARQ or ECC schemes. Accordingly, packet loss rate for end-to-end in a h-hop scenario assuming each node transmission is independent of the other as per the TDMA based MAC protocol in ***Section V.C***

$$E(Tr, h) = \frac{h}{(1 - P_e)} \quad (7)$$

Proof: See [4].

3) REDUNDANT RESIDUE ARITHMETIC BASED ERROR CORRECTION SCHEME

A residue number system (RNS) is a non-weighted number system that uses relatively prime bases as moduli set over GF (2^b) [25]. Owing to the inherent parallelism of its structure and its fault tolerance capabilities, shows fast computation capability and reliability. RNS is defined by a set of β moduli $m_1, m_2, ...m_\beta$, which are relatively prime to each other. Consider an integer data A, which can be represented in its residues $\Gamma_1, \Gamma_2, ...\Gamma_\beta$

$$\Gamma_i = A \ mod \ m_i, \quad i=1,2,....l \quad (8)$$

$$\Theta = \prod_{i=1}^{\beta} m_i \quad (9)$$

The maximum operating range of the RNS is Θ given by (9). The corresponding integer A can be recovered at the decoder side from its β residues by using the Chinese Remainder Theorem [25] as

$$A = \sum_{i=1}^{l} \Gamma_i \times M_i^{-1} \times M_i \tag{10}$$

where $M_i = \Theta/m_i$ and the integers M_i^{-1} are the multiplicative inverses of M_i and computed apriori. One common modulus set $(2^{b-1}-1, 2^{b-1}, 2^{b-1}+1)$ with a power of two in the set makes it relatively easy to implement efficient arithmetic units. A redundant residue number system (RRNS) is defined as a RNS system with redundant moduli. In RRNS, the integer data X is converted in β non-redundant residues and δ-β redundant residues. The operating range Θ remains the same and the moduli satisfy the condition $m_1 < m_2 < .... < m_\beta < m_{\beta+1} < m_{\beta+2} < .... < m_\delta$. RRNS can correct up to $\lfloor(\delta-\beta)/2\rfloor$ errors. If we consider the popular modulus set, mentioned above, and add the redundant modulus (2^b+1) to it, becomes the $(2^{b-1}-1, 2^{b-1}; 2^{b-1}+1, 2^b+1)$ RRNS with capability to detect one error, it is explained extensively in [25]. Since the Chinese Remainder Theorem approach require processing large-valued integers, a suitable method for avoiding this is invoking the so-called base-extension (BEX) method using mixed radix conversion (MRC) [26] that reduces the computation overhead by minimum distance decoding.

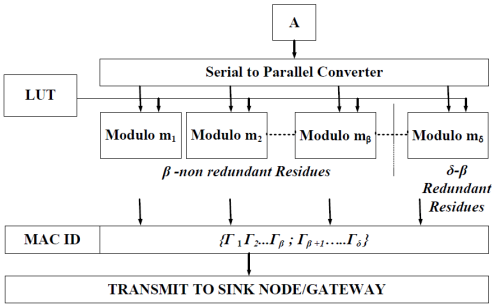

FIGURE 2. RRNS encoding process.

Based on RRNS, we propose an online error detection and correction scheme for the GWSN systems. Fig. 2 shows the encoding process of the data A at the sensor node. A parallel to serial converter changes A into its decimal representation. In a look-up-table (LUT), we store the modulus values of numbers $0-9$ and 10^χ ($\chi \in 1, 2, ...\kappa$) with respect to the δ moduli (β non redundant moduli and δ-β redundant moduli). All operations are performed in parallel modulo channels without the need of transmission of information from one modulo channel to another. So, for 1 moduli, we have δ modulo channels operating in parallel, all operations in each performs modulo of the particular modulus till δ. Finally, we append the respective **MAC IDs** of the sensor devices at the front end of each set of packet data and transmit it to the gateway/sink node. **Algorithm 1** shows the decoding process

Algorithm 1 Algorithm For RRNS Decoding

Inputs: $[y_1, y_2, ...]$
Output: A
$Iter = \binom{\delta}{\beta}$
$Range = \Theta$
$ROM(I,:)$=store all possible combinations of $\binom{\delta}{\beta}$
% Initialize All Parameters
$M = 0$
$X_C(0) = 0$
% Algorithm Starts
for $I = 1$ *to* $Iter$
  $Y_C(I,:) = ROM(I,:)$
% Calculate Current Range
  for $J = 1$ *to* β
    $M = \Theta(I,J)$
  end
% Calculate X
  for $K = 1$ *to* β
    $X_C(K) = X_C(K-1) + \Theta(I,k) * M_k^{-1} * M_k$
  end
% Calculate Possible A
  $A_C(I) = X_C(K)\%M$
end
% Find Error and Decode Input
for $I = 1$ *to* $Iter$
  if $A_C(I) < \Theta$
% mode finds the maximum number
% of times $A_C(I)$ occurs
    $A = mode(A_C(I))$
  end
end

at the sink node/gateway. As can be seen, it first receives the packet and tries to recover the data. After the recovery of the data and the error moduli, it appends a 1-bit **TRUE** flag with the *ACK* signal and sends it to the sensor node to notify the reception of data, else it sends a 1-bit **FALSE** flag with *ACK* to the sensor node signifying to resend the packet data again. The sensor node in turn transmits the δ-β redundant residues again instead of sending the full n bits of data again.

4) PACKET LOSS STATISTICS FOR DIFFERENT ERROR CORRECTING SCHEMES

We perform a theoretical analysis to find out the packet loss rate of the IEEE 802.15.4 based sensor. The systems signal to noise ratio is varied from 0dB to 20dB. The packet error rate is generated for BCH (128, 57, 11) and RRNS (128, 60, 32). These values of n are taken to correlate with the packet load of 133 bits (payload of 127 bits and 6 bits of header). From Fig. 3(a), it can be inferred that ECC schemes provide approximately a gain of 4 dB in SNR as compared to ARQ scheme for the same packet loss rate. This is equivalent to a power gain of around 2 watts, which is essential savings in case of energy constrained GWSN systems. RRNS code provides slightly better gain of around 2 dB, owing to its better error correction capability compared to BCH code. Accordingly, in Fig. 3(b) we plot the values of re-transmissions required for ARQ, BCH codes, and RRNS codes. The plot depicts a similar nature as predicted in (5). As we can see, simple ARQ scheme in a packet loss rate varying from 0 to 20% requires expected number of re-transmissions of $\sim$ 1 to 17, whereas expected number of re-transmissions in BCH and RRNS coding schemes is $\sim$ 1 to 4. The figure of merit for both BCH and RRNS shows expected number of expected packet re-transmissions, even for a packet loss of 20% as ≈ 4, significantly outperforms the simple ARQ scheme. This can save a tremendous amount of energy leading to network lifetime enhancement.

Table 2 analyzes the different BCH schemes and corresponding RRNS schemes. For BCH ($n = 63; k = 16; e = 11$), the error correction capability is 11 bits of

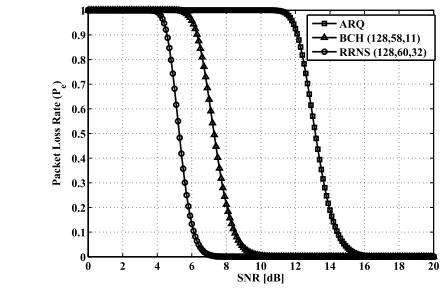

(a)

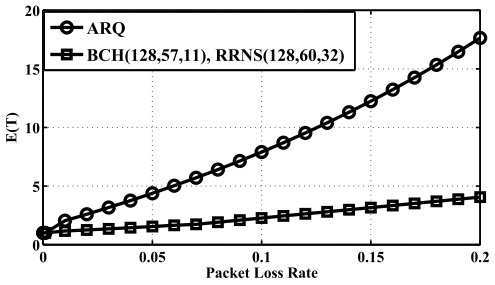

(b)

FIGURE 3. Analytical results of different coding schemes for IEEE 802.15.4 based sensor. (a) Packet loss versus SNR for IEEE 802.15.4 based sensor at different coding schemes. (b) Plot of Expected No. of Packet Re-transmissions versus packet loss rate at different coding schemes for IEEE 802.15.4 based sensor.

TABLE 2. Comparison of RRNS and BCH schemes.

Scheme Details	n	k	Error Correction	Code Rate
BCH $(n = 63; k = 16; e = 11)$	63	16	11-bits	0.254
RRNS $(2^{14} - 1, 2^{14}; 2^{14} + 1, 2^{15} - 1)$	64	28	16-bits	0.438
BCH $(n = 127; k = 57; e = 11)$	127	57	11-bits	0.449
RRNS $(2^{30} - 1, 2^{30}; 2^{30} + 1, 2^{31} - 1)$	128	60	32-bits	0.469
BCH $(n = 127; k = 8; e = 31)$	127	8	31-bits	0.063

errors in a burst of 63 bits data packet. Whereas, in RRNS with 2 redundant moduli $(2^{14} - 1, 2^{14}; 2^{14} + 1, 2^{15} - 1)$ $(n = 64; k = 28; e = 16)$, the error correction capability is 16 bits in a burst of 64 bits data packet. Moreover, the code redundancy is less and code rate is smaller as compared to the corresponding BCH code.

Similarly, in RRNS code with residues $(2^{30} - 1, 2^{30}; 2^{30} + 1, 2^{31} - 1)(n = 128; k = 60; e = 32)$, the error correction capability is 32 bits in a burst of 128 bits. Whereas, in a similar BCH code of $(n = 127; k = 57; e = 11)$, the error correction capability is way less at 11 bits in 127 bits of packet data. If we consider BCH codes with similar error correction capability $(n = 127; k = 8; e = 31)$, the code efficiency is very poor, around $\approx 6.3\%$, as compared to $\approx 47\%$ in RRNS. Thus RRNS code simultaneously shows better efficiency and error correction capability as compared to the BCH and ARQ codes.

5) NETWORK LIFETIME MAXIMIZATION THROUGH ENERGY COST MODEL

By applying RRNS ECC scheme, the optimization problem has been modified here. The processing energy E_{PR} in (11) increases with redundancy $P' = (n - k)/k$. The re-transmissions consumes extra energy resources apart from the original transmission which is mandatory, hence incorporating the expected number of retransmissions $E(Tr, h_i)$ for h_i-hops into (11), we get power consumption as in time slot t

$$\begin{aligned} P_i(P_e, h_i, t) = & \sum_{i\in N, j\in N_i} r_{ij}(t)E_{TX}(t)(1 + E(Tr, h_i)) \\ & + \sum_{i\in N, j\in N_i} r_{ji}(t)E_{RX}(t)(1 + E(Tr, h_i)) \\ & + \sum_{i\in N, j\in N_i} R_{ij}(t)E_{PR}(t)(1 + E(Tr, h_i)P') \\ & + \sum_{i\in N, j\in N_i} R_{ij}(t)E_{SN}(t) + \sum_{l\in O(i)} P_{LS}(t) \end{aligned} \quad (11)$$

packet success rate $P_s(t)$ affects the sample rate in the rate flow constraint as

$$\sum_{j\in N_i}\sum_{t=1}^{T_i} \left(r_{ij}(t) - r_{ji}(t) + P_s(t)R_{ij}(t)\right) \le 0, \ \forall i \in N, j \in N_i \quad (12)$$

The problem of maximizing the network lifetime can be stated as

$$\begin{aligned} & \max_{t\ge 0, E_B(t)>0} \ T_i \\ & \textbf{subject to} \ \sum_{t=1}^{T_i} (P_i(P_e, h_i, t)) \le \frac{1}{T_i} \cdot E_B(t), \\ & \sum_{j\in N_i}\sum_{t=1}^{T_i} \left(r_{ji}(t) - r_{ij}(t) - P_s(t)R_{ij}(t)\right) \le 0, \\ & \forall i \in N, \quad j \in N_i \\ & E_{TX} = a_1 + a_2 \cdot d^{\gamma}, \quad \gamma \in [2, 6] \\ & 0 \le r_{ij} \le C_l \end{aligned} \quad (13)$$

In our model, we have considered a battery with a finite maximum capacity E_{Bmax}, where $E_B(t) \le E_{Bmax}$. Further, due to hardware limitations the total power consumption is upper bounded by maximum consumption P_{max} (i.e $P_i(t) < P_{max}$, $\forall j \in N_i, \forall t \in T_i$). Problem in (13) is not convex. By substituting $s = 1/T$, we obtain a convex maximization problem in s.

$$\begin{aligned} & \min_{s\ge 0} \ s_i \\ & \textbf{subject to} \ \sum_{t=1}^{T_i} (P_i(P_e, h_i, t)) \le s_i \cdot E_B(t), \ 1 \le t \le T_i \\ & 0 < E_B(t) \le E_{Bmax}, \ 1 \le t \le T_i \\ & \text{Constraints in (13)} \end{aligned} \quad (14)$$

V. WIRELESS ENERGY HARVESTING AND WAKE-UP RADIO SCHEME

A critical challenge in large scale implementation of WSNs technology and in a greater scope, IoT, is providing energy to the nodes. A more attractive energy harvesting approach is wireless (RF) energy harvesting which provides key advantages in virtue of being controllable, lower cost and smaller form factor implementation [15], [27]. In this section, enabling technologies for efficient wireless energy harvesting is presented. Also, an energy-efficient method to decrease the power consumption of nodes during the receive mode is discussed.

A. WIRELESS ENERGY HARVESTING NETWORKS

The wireless energy harvesting unit is in charge of receiving the transmitted waves and efficiently converting them into a stable waveform to recharge or to supply the node. In the context of our system, the wireless energy sources fall into two categories of *dedicated sources* and *Ambient sources* [27]. A dedicated RF source is deliberately deployed to supply energy to the nodes at a designated rate and optimum frequency (e.g., sink node). An example of a dedicated source is the sink node in our system model. An ambient source, on the other hand, is a less predictable energy source happens to exist within the operation area of the network [28], but are not designed as a part of the network. Examples of ambient sources include TV and radio towers (static ambient source) and WiFi access points (dynamic ambient source). Due to their unpredictable nature, harvesting energy from ambient sources is an opportunistic process which requires some level of adaptivity and entails a more sophisticated design both at circuit and system levels. Block diagram of a generic wireless energy harvesting (WEH) enabled sensor node is shown in Fig. 4. As shown in the figure, the nodes consists a rectifier, transceiver (RX, TX), sensors and sensor interface, storage unit (rechargeable battery), power management unit (PMU) and the processor. An RF-to-DC converter (also known as rectifier) constitute the core of the wireless energy harvesting unit. The rectifier is in charge of converting the received RF power to a usable DC supply. The conversion from RF to DC comes with some energy loss in the internal circuitry of the rectifier which quantified in terms of power conversion efficiency (PCE) of the rectifier. PCE being the ratio of the converted DC power to the RF input power, has significant implications on the overall performance of the power harvesting unit with reference to reference to Friis free space equation which gives the available harvested power by [29]

$$P_H = P_{TX} \cdot P_L \cdot G_{TX} \cdot G_{RX} \cdot PCE \cdot \frac{\lambda^2}{(4\pi d)^2} \qquad (15)$$

where P_H is the available harvested power, P_{TX} is the transmitted power by the source, P_L is the path loss, G_{TX} is the transmitter antenna gain, G_{RX} is the receiver (node) antenna gain, PCE is power conversion efficiency of the rectifier, λ is the wavelength of the transmitted wave and d is the communication distance. In most applications, the

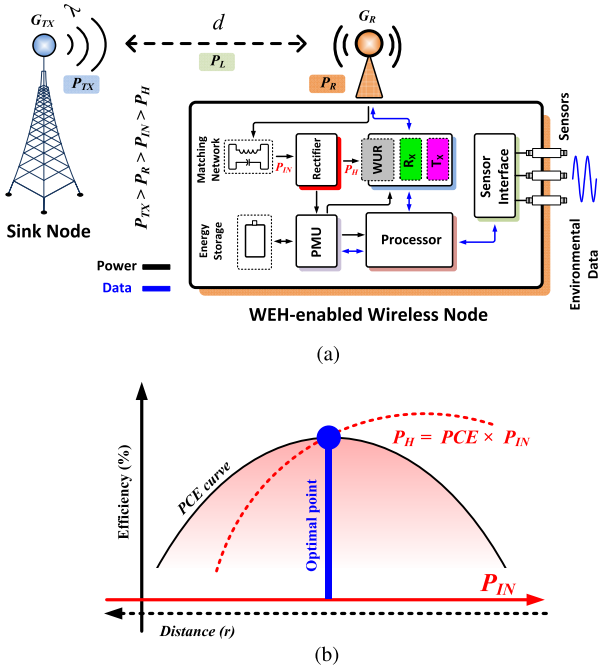

FIGURE 4. WEH-enabled wireless sensor node. (a) Block diagram of WEH-enabled sensor node. (b) Efficiency curve of the rectifier versus communication distance.

RF transmitters are subject to regulatory requirements (in terms of frequency and maximum transmitted power), antenna gains are set by geometry obligations and the distance set by the network specification. All these limitations render the PCE as the only viable design parameter to enhance the performance of the WEH unit and consequently prolong the life time of the network nodes [30]. The PCE is optimized for a designated input power which corresponds to an specific communication distance. For longer (than optimal) distances (d_{ij}^2), the rectified power abruptly drops. When a receiver node i is in the energy harvesting mode, the power harvested (P_{H_i}) from base station server source in a time slot t can be calculated as follows

$$P_{H_i}(t) = \frac{\eta \cdot P_{TX} \cdot |H_i(t)|^2}{d_{ij}^2}, 1 \le t \le T_i \qquad (16)$$

Where, η is PCE and H_i denotes the channel gain between between source and receiver at time slot t. As shown, the PCE is optimized for a designated input power (received form the antenna) which corresponds to an specific communication distance. Beyond this optimal point, the rectifier provides sufficient energy for storage or to drive the node circuitry. However, for longer distances from the sink node, the rectified power abruptly drops. In WEH-enabled nodes, PMU is in charge of managing the flow of energy to the storage unit, node circuitry and to the main receiver (RX). Aside from high efficiency, other key performance metrics of a WEH unit include high sensitivity (i.e., ability to harvest energy from small levels input power), wide dynamic range (i.e., maintaining high efficiency for a wide range of input powers), multi-band operation (i.e., ability to harvest wireless energy

from wireless transmissions at different frequencies). Extensive studies exist in the literature investigating on techniques to improve the performance of WEH unit [27], [29]. The design presented in [31] studies techniques to enhance the efficiency of WEH unit and a muliti-band approach to enable harvesting and different frequencies.

B. WAKE-UP RADIO SCHEME

In a wireless sensor node, the receiver unit despite not being the most power hungry block, constitutes a significant portion of the overall energy consumption of the system. While similar to other building blocks, the receiver is practically called in to action only when its service is required. It has to keep listening to the communication channel for the commands from the sink node. An efficient solution to tackle the energy consumption during the idle listening mode is duty cycling (also known as *rendez-vous* scheme) in which the receiver maintains in deep sleep mode and only wakes up when there is a message to be received from the main transmitter (TX). There are three main classes of duty cycling, namely, synchronous, pseudo-asynchronous and asynchronous [32]. In the synchronous scheme, the transmitter and all the receivers pre-schedule designated time slots in which the receivers wake up for to receive the commands and fulfill the transmission. Such scheme imposes considerable overhead in terms of complexity and power consumption in order to establish time synchronization and leads to idle energy consumption if there is no data to be received during the pre-scheduled time slots. In the pseudo-asynchronous scheme, the receivers wake up at designated time but a synchronization between the transmitter and receiver is not required. In the asynchronous scheme which the most energy efficient approach among the duty-cycling classes, the receivers spends most of their time in deep sleep mode and only wake up when interrupted by the transmitter. This interrupt message is generated by a wake-up radio (WUR). WUR is a simple and low-power receiver which keeps listening to the channel and only wakes up the main receiver when the is a request for transmission to the associated node [33]. This so called *listening* mode power (P_{LS}) consumption when integrated over the lifetime of the node is dependent on the amount of network utilized for given duty cycle. Let $\alpha \in (0, 1)$ be the system parameter that defines the amount of network utilization. The amount of energy consumption modeled in terms of α in (11) is

$$\begin{aligned} P_i(P_e, h_i, t) = & \sum_{i\in N, j\in N_i} r_{ij}(t)E_{TX}(t)(1 + E(Tr, h_i)) \\ & + \sum_{i\in N, j\in N_i} r_{ji}(t)E_{RX}(t)(1 + E(Tr, h_i)) \\ & + \sum_{i\in N, j\in N_i} R_{ij}(t)E_{PR}(t)(1 + E(Tr, h_i)P^{'}) \\ & + \sum_{i\in N, j\in N_i} R_{ij}(t)E_{SN}(t) + \sum_{l\in O(i)} \alpha(t)P_{LS}(t) \end{aligned} \tag{17}$$

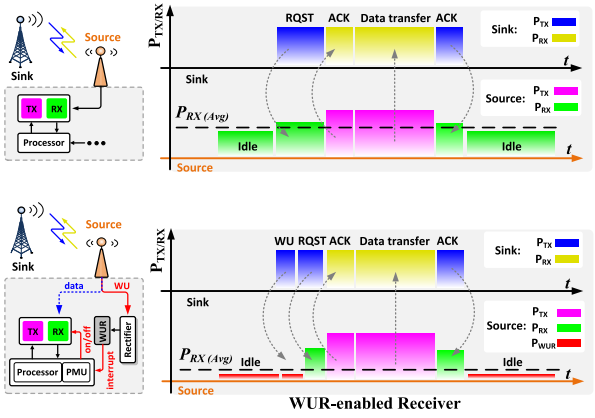

(a)

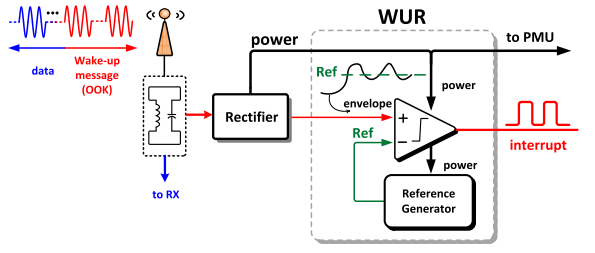

(b)

FIGURE 5. WUR-enabled wireless sensor node. (a) Timing diagram of conventional and WUR-enabled receivers. (b) Block diagram of WUR unit.

Fig. 5 schematically compares the energy profile of a conventional transceiver versus that of a WUR-enabled transceiver. As shown in the figure, as compared to the conventional method, the main receiver (RX) in the WUR-enabled transceiver is activated only upon receipt of the wake-up command (WU) which is followed by the interrupt message generated by the WUR. The infrequent activation of RX facilitates a substantial energy conservation over the life-time of the wireless node. Obviously, WUR scheme is favourable only if the power consumption of the WUR is much smaller than that of RX (i.e., $P_{WUR} \ll P_{RX}$ in Fig. 5(a)). WEH-enabled nodes provide a good opportunity for a very efficient implementation of WUR [34]. Fig. 5(b), shows the block diagram of one such implementation for on-off keying (OOK) WU message. As shown in the figure, the rectifier block of the WEH unit can be re-utilized to perform as a simple envelope detector while also providing energy supply for the rest of WUR circuitry [34].

C. MEDIUM ACCESS CONTROL FOR WEH-WSN

In this section, the MAC protocols for WSN is presented which complements our wake-up radio design. MAC protocols for WSNs can be classified under contention-based and contention free schemes which are further divided into *scheduled, random access, and duty-cycle based* schemes. In scheduled MAC protocols (e.g, [35]), time slots are being assigned for each node to transmit so that idle listening mode can be eliminated, and collision can be avoided.

However, this exchange requires additional overhead as well as a synchronization in time with a global clock, which is very tough to attain. Since the energy source is unpredictable in WEH-WSNs, it is difficult for nodes to exchange time schedules as they do not know future energy availability. Random access protocols also called contention based protocols, do not need to exchange schedules but incur additional idle time for the node to sense the channel before transmitting (like CSMA/CA schemes), and overhearing time to listen to packets not destined to itself (S-MAC, B-MAC) [35]. MAC protocols based on Time Division Multiple Access (TDMA) with wakeup and sleep periods have attracted considerable interest because of their low power consumption and collision free operation [36], [37], [38]. Due to its benefits of reduced collisions, scalability and bounded latency, TDMA is widely considered in wireless networks. TDMA partitions time into many fixed slots and nodes transmit data in their assigned slots, thereby avoiding collisions. The duty cycling concept is greatly efficient in terms of power saving. TDMA based protocols are more energy efficient, and the energy consumed is proportional to the length of the transmission cycle while the latency is proportional to the size of the network. Moreover, a single global clock is not needed for synchronization in wake-up duty cycled TDMA schemes.

ODMAC, an on-demand MAC protocol, was proposed to support individual duty cycles letting the nodes operate in the energy neutral operation state by exploiting the maximum harvested energy [36]. This state guarantees infinite lifetime as soon as there are not any hardware failures. However, it is hard to design the sensors to be always in this state since the dynamics of the environmental energy sources are hard to predict. It exploits the fact that sensor nodes often have low traffic in order to remove the burden of idle listening by Carrier Sensing. A drawback of ODMAC is the lack of retransmissions, so the successful reception of packets is not acknowledged, which might result in discarding all the packets involved in collisions. Some other protocols proposed for EH-WSN are EH-MAC and ERI-MAC [37]. EH-MAC is an ID-polling-based MAC protocol proposed for multihop EH-WSNs and it achieves high channel perfor- mance in terms of network throughput and fairness. ERI-MAC is a receiver initiated protocol which dynamically adjusts the duty-cycle based on the energy harvesting state of the system.

To cater for the interference in the TDMA MAC model, our analysis is based on WUR scheme for low power duty cycling with transmission capacity provided with the incorporation of ECC codes.

D. MODELING ENERGY HARVESTING AND WAKE-UP RADIO

Let $P^C_{H_i}(t)$, denotes the cumulated harvested energy in all the slots of node i. For simplicity, we assume the harvested energy is available at the start of each interval t. We also assume that the battery has finite capacity and harvested energy can only recharge till the maximum capacity of battery E_{Bmax}.

$$P^C_{H_i}(t) = \sum_{x=1}^{t} P_{H_i}(x), (t \in 1, 2, ...T_j) \tag{18}$$

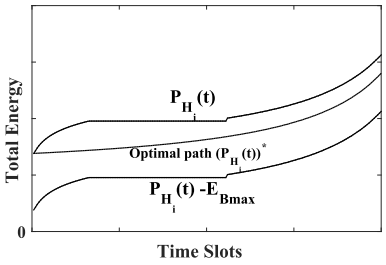

FIGURE 6. Feasible energy bound for harvested energy.

$P^C_{H_i}(t)$ is a continuous increasing function that lies between points (0, 0) and $(T_j, P^C_{H_i}(T_j))$ as shown in Fig. 6. The cumulative node energy $P^C_i(t)$ for all $(t \in 1, 2, ...T_j)$ cannot be more than $P^C_{H_i}(t)$. Using this constraint, the dynamic charging and discharging of battery can be modeled as

$$\begin{aligned} E_B(t+1) &= E_B(t) - P_i(t) + P_{H_i}(t) \\ P^C_i(t) &\le P^C_{H_i}(t), \forall t \in 1, 2, ...T_j \end{aligned} \tag{19}$$

To find an optimal energy consumption $(P^C_i(t))^*$, we need to find the upper and lower bound of consumed energy. (19) gives the upper bound on the consumed energy. Further, $(P^C_i(t))^*$ must satisfy that, the residual energy of nodes at all time slots i.e. $(P^C_i(t))^* - P^C_{H_i}(t)$ cannot exceed the battery maximum capacity E_{Bmax}, forms the lower bound of $(P^C_i(t))^*$. Thus the problem in (14), can be reformulated as

$$\begin{aligned} &\textbf{min}\ s_i \\ &s{\ge}0 \\ &\textbf{subject to}\ \sum_{t=1}^{T_i} \big(P_i(P_e, h_i, t) - s_i \cdot E_B(t) - P_{H_i}(t)\big) \le 0, \\ &\quad 1 \le t \le T_i \\ &\quad 0 < E_B(t) \le E_{Bmax}, \quad 1 \le t \le T_i \\ &\quad P^C_{H_i}(t) - E_{Bmax} \le P^C_i(t) \le P^C_{H_i}(t), \\ &\quad \forall t \in 1, 2, ...T_i \\ &\quad \text{Constraints in (13), (16), (17) and (18)} \end{aligned} \tag{20}$$

VI. JOINT UTILITY & NETWORK LIFETIME TRADE-OFF AND DISTRIBUTED SOLUTION

Solving standalone maximization of network lifetime problem by varying the source rates will result in allocation of zero source rates to the node. Thus, it results in application performance of the system to be worst. Therefore, it is optimal to jointly maximize the network lifetime with the system's application performance. We associate the network performance with the utility function $U_i(.)$. In [3], it has shown that each node $i{\in}N$ is related to a utility function and achieve different kind of fairness by maximizing the network utility. Thus the utility is a function of the node source rate R_{ij}. Apart from source rates, packet success rate P_s also affects

the overall system performance. Thus, the utility function has to be modified to accommodate the packet success rate and the payload data efficiency as $U_i(R_{ij}, P_s)$. Max-Min fairness maximizes the smallest rate in the network whereas the Proportional fairness favors the nodes nearer to the sink node. As given in [3], by aggregating the utility, the network lifetime can be solved in a distributed way with an approximated approach as $F_s^{\epsilon}(.) = \left(\frac{1}{\epsilon+1}\right) \cdot s_i^{\epsilon+1}$. Thus, the network lifetime problem in (20) becomes

$$\begin{aligned} &\min_{s\geq 0} \left(\frac{1}{\epsilon+1}\right) \cdot s_i^{\epsilon+1} \\ &\textbf{subject to} \text{ constraints in (20), (17) \& (12)} \end{aligned} \tag{21}$$

Using (21), we can now formulate a joint trade-off between maximizing utility and network lifetime simultaneously. Our method differs from other approaches in **Section II** as we consider a more practical scenario, incorporating path loss, fairness, packet loss statistics for error control schemes as well as energy harvesting and a event driven radio wake-up scheme. Thus the cross-layer joint maximization problem is given as

$$\begin{aligned} &\max_{(s,R_{ij},r_{ij})\geq 0} \sum_{t=1}^{T_i} \alpha(t) \sum_{i\in N} \sum_{j\in N_i} U_i(R_{ij}(t), P_s(t)) \\ &\qquad - \sum_{t=1}^{T_i} (1-\alpha(t)) \left(\frac{1}{\epsilon+1}\right) \cdot s_i^{\epsilon+1} \\ &\textbf{subject to} \text{ constraints in (20), (17) \& (12)} \end{aligned} \tag{22}$$

We have introduced a system parameter $\alpha \in [0, 1]$ in (17). It gives the trade-off between the utility and network lifetime. For α=0, the utility is zero and for α=1, network lifetime is maximum with worst application performance. The maximization objective function is concave as $U(.)$ is concave and network lifetime problem $F_s^{\epsilon}(.)$ is convex. We try to solve the primal problem via solving the dual problem [22]. We keep the expected number of transmissions $E(Tr, h_i)$ in hops h_i as constant and vary the rate r_{ij}. The constraint set in (22) represents a convex set. According to slater's condition for strong duality, if the non-linear constraints are strictly positive, duality gap between primal and dual problem is small. Thus the primal can be solved by solving the dual problem and the desired primal variables can be obtained. The dual-based approach leads to an efficient distributed algorithm.

A. DUAL PROBLEM

To solve the problem in a distributed manner, we formulate the Lagrangian in terms of the Lagrange Multipliers λ and μ by relaxing the inequality constraints in (22).

$$\begin{aligned} &\mathbf{L}(\lambda, \mu, \mathbf{s}, \mathbf{r_{ij}}, \mathbf{R_{ij}}, \mathbf{U(R_{ij}, P_s)}, \mathbf{t}) \\ &= \sum_{t=1}^{T_i} \alpha(t) \sum_{i\in N} \sum_{j\in N_i} U_i(R_{ij}(t), P_s(t)) \\ &\quad - \sum_{t=1}^{T_i} (1-\alpha(t)) \left(\frac{1}{\epsilon+1}\right) \cdot s_i^{\epsilon+1} \\ &\quad + \sum_{j\in N_i} \sum_{t=1}^{T_i} \lambda_l(t)\big(r_{ij}(t) - r_{ji}(t) + P_s(t)R_{ij}(t)\big) \\ &\quad + \sum_{i\in N} \sum_{j\in N_i} \sum_{t=1}^{T_i} \mu_i(t)\big(P_i(P_e, h_i, t) - s_i \cdot E_B(t) - P_{H_i}(t)\big) \end{aligned} \tag{23}$$

The corresponding Lagrange dual function $D(\lambda, \mu)$ and the solution F^* is given by

$$\begin{aligned} \mathbf{D}(\lambda, \mu) = &\sup_{s, r_{ij}, R_{ij}, U} L(\lambda, \mu, s, r_{ij}, R_{ij}, U(R_{ij}, P_s), t) \\ &\textbf{subject to} \text{ constraints in (20), (17) \& (12)} \end{aligned} \tag{24}$$

$$\mathbf{F}^* = \min_{\lambda>0, \mu>0} \mathbf{D}(\lambda, \mu) \tag{25}$$

The dual problem of (24) can be decomposed further into two different subproblems $D_1(\lambda, \mu)$ and $D_2(\lambda, \mu)$. Subproblem $\mathbf{D_1}(\lambda, \mu)$ is a rate control problem in the network and transport layer of the sensor networks. For all active links $l \in L$, we substituted $\sum_{i\in L}$ with $\sum_{i\in N} \sum_{j\in N_i}$. Subproblem $\mathbf{D_2}(\lambda, \mu)$ gives the bound on the inverse lifetime. The objective function of the primal problem is not strictly convex in all its primal variables $\{s, R_{ij}, r_{ij}\}$. The sub-dual problems $\mathbf{D_1}(\lambda, \mu)$ is only piecewise differentiable. Therefore, the gradient projection method cannot be used to solve the problem. We use the subgradient method [22] to solve the problem iteratively till a desirable convergence is reached.

$$\begin{aligned} &\mathbf{D_1}(\lambda, \mu) \\ &= \max_{(R_{ij}, r_{ij})\geq 0} \sum_{i\in N} \sum_{j\in N_i} \sum_{t=1}^{T_i} \alpha(t) \cdot U_i(R_{ij}(t), P_s(t)) \\ &\quad + \sum_{l\in L} \sum_{t=1}^{T_i} \lambda_l(t)\big(r_{ij}(t) - r_{ji}(t) + P_s(t)R_{ij}(t)\big) \\ &\quad + \sum_{i\in N} \sum_{j\in N_i} \sum_{t=1}^{T_i} \mu_i(t) \cdot \big(r_{ij}(t)E_{TX}(t)(1 + E(Tr, h_i))\big) \\ &\quad + \sum_{i\in N} \sum_{j\in N_i} \sum_{t=1}^{T_i} \mu_i(t) \cdot \big(r_{ji}(t)E_{RX}(t)(1 + E(Tr, h_i))\big) \\ &\quad + \sum_{i\in N} \sum_{j\in N_i} \sum_{t=1}^{T_i} \mu_i(t) \cdot \Big(R_{ij}(t)E_{PR}(t)(1 + E(Tr, h_i)P^{'})\Big) \\ &\quad + \sum_{i\in N} \sum_{j\in N_i} \sum_{t=1}^{T_i} \mu_i(t) \cdot \big(R_{ij}(t)E_{SN}(t) + \alpha(t)P_{LS}(t)\big) \\ &\textbf{subject to} \\ &\quad E_{TX} = a_1 + a_2 \cdot d^{\gamma}, \quad \gamma \in [2, 6] \\ &\quad 0 \leq r_{ij} \leq C_l \\ &\quad P_{H_i}^C(t) - E_{Bmax} \leq P_i^C(t) \leq P_{H_i}^C(t), \quad \forall t \in 1, 2, ...T_i \end{aligned} \tag{26}$$

$$\mathbf{D_2}(\lambda, \mu)$$
$$= -\{ \max_{(s,E_B)\geq 0} \sum_{i\in N} \sum_{j\in N_i} \sum_{t=1}^{T_i} \mu_t \left(s_i \cdot E_B(t) + P_{H_i}(t)\right)$$
$$+ \sum_{t=1}^{T_i} (1-\alpha(t)) \left(\frac{1}{\epsilon+1}\right) \cdot s_i^{\epsilon+1} \}$$

subject to

$$0 < E_B(t) \leq E_{Bmax}, 1 \leq t \leq T_i$$
$$P^C_{H_i}(t) - E_{Bmax} \leq P^C_i(t) \leq P^C_{H_i}(t), \forall t \in 1, 2, ...T_i \quad (27)$$

Let, $s^*(\lambda, \mu), R^*_{ij}(\lambda, \mu), r^*_{ij}(\lambda, \mu), (P^C_{H_i}(t))^*, \ P^*_s(t), P^*_{LS}(t)$ be the optimal solutions for problems (26) and (27). We define the following to obtain the distributed solution,

Definition 1: Let f:$\Re^n \to \Re$ is a convex function. The sub-gradient of f at a point x'$\in \Re^n$ satisfy the following inequality with respect to a point y'$\in \Re^n$, ($\nabla f(x')^T$ is the gradient of f at x')

$$f\left(y'\right) \geq f\left(x'\right) + \left(y' - x'\right) \nabla f(x')^T \quad (28)$$

Using **Definition 1**, we write the update for dual variables at the $(\tau+1)^{th}$ iteration as,

$$\lambda_l\left(t, \tau+1\right) = \left[\lambda_l\left(t, \tau\right) + \varphi_\tau \nabla_\lambda D(\lambda, \mu)^T\right]^+,$$
$$\mu_i\left(t, \tau+1\right) = \left[\mu_i\left(t, \tau\right) + \psi_\tau \nabla_\mu D(\lambda, \mu)^T\right]^+ \quad (29)$$

$[.]^+$ is the projection on the non-negative orthant meaning z^+=max{0, z}, $\{\varphi_\tau, \psi_\tau\}$ are the positive step sizes and $\{\nabla_\lambda D(\lambda, \mu), \nabla_\mu D(\lambda, \mu)\}$ are the gradients of dual problem in (25) w.r.t λ and μ.

B. SOLUTION TO GWSN DISTRIBUTED ALGORITHM AND ITS CONVERGENCE ANALYSIS

The Lagrange multipliers (λ_l, μ_i) have cost interpretation to them. λ_l represents the link capacity cost and μ_i denotes the battery utilization cost of sensor node i. The gradients $\nabla_\lambda D(\lambda, \mu)$ and $\nabla_\mu D(\lambda, \mu)$ denote the excess link capacity and battery energy respectively. Problems $\mathbf{D_1}(\lambda, \mu)$ in (26) represent the maximization of the aggregate utility of the network in presence of flow constraints and energy spent in the network. The network lifetime problem $\mathbf{D_2}(\lambda, \mu)$ in (27) maximizes the revenue from battery capacities subtracting the lifetime-penalty function, resulting in reduction of lifetime. The procedure for solving the **GWSN Algorithm 2** is outlined as follows:

Now we discuss the convergence of our distributed algorithm for GWSN. It is worth noting that the proposed algorithm takes into account the lifetime constraint, energy harvesting constraint, packet loss statistics and path loss into consideration. Thus it is necessary to analyze the convergence bounds.

Lemma 2: When $\epsilon \to \infty$, the network lifetime $T_{network}$ determined by the optimal solution s^* of problem (22) approximates the maximum network lifetime of the wireless sensor network.

Proof: See Appendix A.

Algorithm 2: GWSN Distributed Algorithm

- Initialize all the inputs ($E_{TX}, E_{RX}, E_{SN}, E_{PR}, P_{LS}, E_B$) and step sizes $\varphi_\tau \leftarrow 0.01, \psi_\tau \leftarrow 0.01/\sqrt{\tau}, \epsilon \leftarrow 20$.
- Although the problem in $\mathbf{D_1}(\lambda, \mu)$ and $\mathbf{D_2}(\lambda, \mu)$ is convex, the solution is complex and difficult to implement due to the intricacies introduced by incorporation of optimal energy consumption ($(P^C_i(t))^*$), packet loss ($P^*_s(t)$) and WUR ($P^*_{LS}(t)$). From (26) and (27), it is evident that $(P^C_i(t))^*$ is dependent on optimal lifetime (s^*_{ij}) and sample rate (R^*_{ij}). Therefore we take $(P^C_{H_i}(t))^*$ as some function g of lifetime and sample rate.

$$g(s^*_{ij}, R^*_{ij}) = f((P^C_{H_i}(t))^*) \quad (30)$$

- We model $P^C_{H_i}(t)$ w.r.t the channel gain $H_i(t)$ distributed as *i.i.d* with mean 0. Once the optimal s^*_{ij}, R^*_{ij} is found, $P^C_{H_i}(t)$ is found using $f^{-1}\left(g(s^*_{ij}, R^*_{ij})\right)$.
- The packet success rate $P_s(t)$ is varied $\in$ [80, 100] and system utility parameter $\alpha(t)$ and overall node utilization $U_i(R_{ij}(t), P_s(t))$ determines the optimal listening power $P^*_{LS}(t)$.
- Thus from all the previous assumptions mentioned above, the time coupling property of the node can be excluded and finding solution for $\lim_{t\to 1} \lambda(t)$, $\mu(t)$ would be good $\forall t \in (1, 2, 3, ...T_i)$.
- The Lagrange multipliers can be updated by

$$\lambda_l\left(t, \tau+1\right)$$
$$= [\lambda_l\left(t, \tau\right) + \varphi_\tau \sum_{j\in N_i} \left(r_{ij}(t,\tau) - r_{ji}(t,\tau) + P_s(t,\tau) R_{ij}(t,\tau)\right)]^+,$$
$$\mu_i\left(t, \tau+1\right)$$
$$= [\mu_i\left(t, \tau\right) + \psi_\tau \sum_{i\in N} \sum_{j\in N_i}$$
$$\left(P_i(P_e, h_i, t, \tau) - s_i \cdot E_B(t, \tau) - P_{H_i}(t, \tau)\right)]^+ \quad (31)$$

- From (29), (31), it can be seen that as the flow r_{ij} exceeds the capacity of link C_l, the link cost and node energy cost increases. Thus higher link and node-battery prices result in greater penalty in the objective function in (26) forcing source rates R_{ij} & flows r_{ij} to reduce. Although higher node-battery cost (27) allow greater revenue for the same increase in battery capacities (by increasing 's'), there is a corresponding penalty incurred due to the consequent lower lifetimes.

Further, let us make the following two assumptions as below:

- **Assumption 1**: Let $U_i(R_{ij}, P_s)$ be defined as $log_2(R_{ij}P_s)$ which is an increasing and concave function, and its inverse and hessian exists.
- **Assumption 2**: Hessian of $U_i(R_{ij}, P_s)$ is negative semidefinite and $r^{min}_{ij} \leq r_{ij} \leq r^{max}_{ij}$.

Define $\overline{L}$ = max L as the maximum number of links that a sensor node uses. Let $\overline{U}$ = max $U_i^{'}(R_{ij}, P_s)$ and $\overline{R}$ = max r_{ij}, be the maximum rate flow of the node when transmitting information from $i \to j$.

*Proposition 1: If the assumptions 1 and 2 above hold and the step size satisfies $0 < \varphi_\tau, \psi_\tau < \frac{2}{\overline{L}^{1/2}\overline{U}\,\overline{R}}$. Then starting from any initial rates $r^{min}_{ij} \leq r_{ij} \leq r^{max}_{ij}$, & price $\lambda_l, \mu_i \geq 0$, every limit point of the sequence $\{s(\lambda, \mu), R_{ij}(\lambda, \mu), r_{ij}(\lambda, \mu)\}$ generated by **GWSN Algorithm 2**, is primal-dual optimal.*

Proof: See Appendix B.

Lemma 3: By the above distributed algorithm, dual variables (λ_l, μ_i) converge to the optimal dual solutions (λ^*_l, μ^*_i),

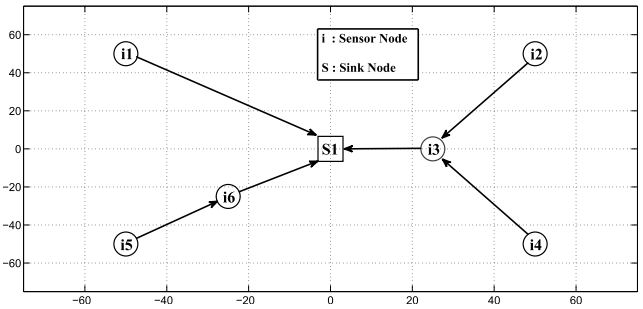

FIGURE 7. WSN topology.

TABLE 3. WSN simulation parameters.

Parameter	Description	Value
a_1	Transceiver Constant	10^{-7} J/bit
a_2	Transceiver Constant	$0.1 \cdot a_1$ J/bit
γ	Path Loss Exponent	4
ϵ	Lifetime Approximation Constant	20
E_{RX}	Receiver energy per bit	$1.35 \cdot 10^{-7}$ J/bit
E_{SN}	Sensing energy per bit	$5 \cdot 10^{-8}$ J/bit
E_{PR}	Processing energy per bit	$5 \cdot 10^{-8}$ J/bit
P_{LS}	listening power	1 mW
E_B	Battery energy of sensor node	1 J

if the stepsizes are chosen such that

$$\varphi_\tau(i) \to 0, \sum_{i=1}^{\infty} \varphi_\tau(i) = \infty, \psi_\tau(i) \to 0, \sum_{i=1}^{\infty} \psi_\tau(i) = \infty \tag{32}$$

VII. SIMULATION RESULTS

To show the joint trade-off between maximizing utility and network lifetime in terms of system parameter α, path loss γ, packet loss statistics $\{P_e^i\}$, energy harvesting P_{H_i}, we consider a WSN as shown in Fig. 7 with seven nodes distributed over a square region of 100m $\times$ 100m. The node at the middle of the network is taken as the sink node and the other six nodes are either source or source/relay nodes. Nodes $\{i1, i2, i4, i5\}$ act as source nodes whereas nodes $\{i3, i6\}$ act as source node to deliver its own data and relay nodes for delivering nearest neighbor's data to the sink node. The parameters taken for the simulation are depicted in Table 3. The value of E_{TX}, $\{a_1, a_2\}$ are chosen from [4] with γ=4. E_{RX} and E_{SN} are taken from [39]. Processing energy E_{PR} is assumed to be same as the sensing energy E_{SN}. Also, at start t_0 the initial battery energy E_B in all the nodes is taken as 1 J. We run our simulations till 500 iterations to get a desired solution for the system.

A. CONVERGENCE PLOTS

To show the convergence of our GWSN algorithm according to **Lemma 2**, and **3**, we plotted in Fig. 8(a), the convergence of source node rates for different sensor nodes with respect

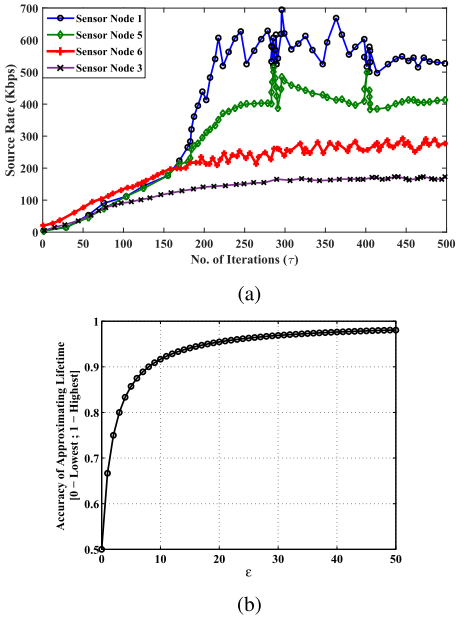

FIGURE 8. Simulation plots of convergence of GWSN algorithm. (a) Convergence of source node rates for different sensor nodes with respect to the number of iterations with $\alpha = 0.1$. (b) Error in measuring the lifetime with respect to the lifetime approximation coefficient.

to the number of iterations. We have chosen sensor node $\{i1, i3, i5, i6\}$, where $\{i1, i5\}$ act as only sensor nodes and $\{i3, i6\}$ act as both sensor and relay node. The step size is taken as $\varphi_\tau = 0.01$, where τ is the index of iteration. It can be observed that the step size plays a vital role as it controls the magnitude of oscillations near the optimal solution. The larger the step size, the faster the convergence but with more variations near the point of optimality whereas smaller step size reach a stable optimal solution with lesser fluctuations near the optimal. As predicted by our algorithm, sensor nodes that have lower lifetime $\{i1, i5\}$ are assigned higher rates, whereas nodes with higher lifetime $\{i3, i6\}$ have lower rates being assigned to them. Fig. 8(b) shows the error in measuring the lifetime with respect to the coefficient ϵ.

$$Error\ in\ Approximating\ Lifetime = \left| s - \frac{1}{\varepsilon + 1} s^{\varepsilon+1} \right| \tag{33}$$

According to **Lemma 2**, if the coefficient ϵ is large enough then the lifetime approximated by (22) is the maximum lifetime. Fig. 8(b) validates the point, as it can be seen that at $\epsilon = 10$, we get less than 10% error in measurement of lifetime. For our Algorithm, we have initialized the value of ϵ as 20 with less than 5% error in lifetime prediction.

B. UTILITY AND LIFETIME TRADE-OFF WITH WEH AND WUR CONSTRAINTS

The impact of the system design parameter $\alpha(t)$ is shown in Fig. 9(a), 9(b) & 9(c). $\alpha(t)$ is varied between 0.1 to 0.9. The network utility is computed as $(\sum_{i=1}^{6} log_2(R_{ij}P_s))$ which is the aggregate utility of all the nodes not including the sink

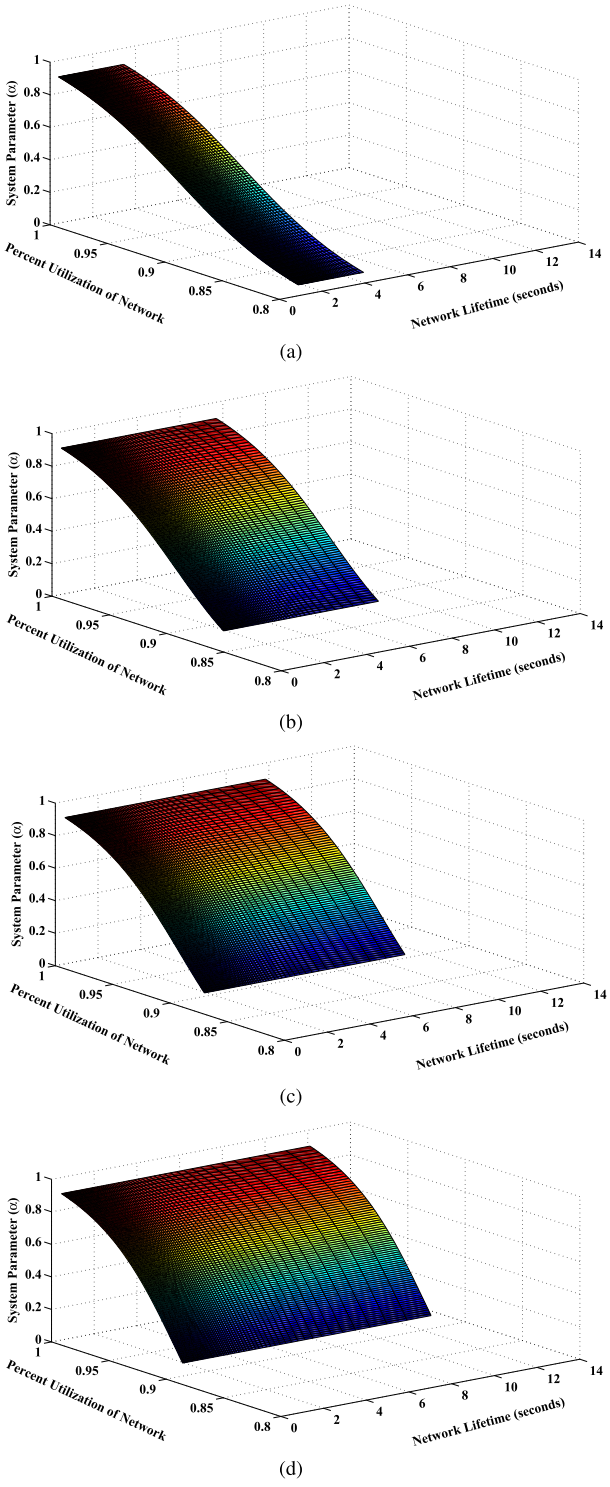

FIGURE 9. Simulation plots of Network Aggregate Utility - Lifetime trade-off for different α. (a) Network Aggregate Utility - Lifetime trade-off without WER, WUR and ECC. (b) Network Aggregate Utility - Lifetime trade-off with WER, and without WUR and ECC. (c) Network Aggregate Utility - Lifetime trade-off with WER and WUR without ECC. (d) Network Aggregate Utility - Lifetime trade-off with WER, WUR & ECC.

node $s1$. The aggregate utility have been normalized with respect to the maximum utility of the network. Fig. 9(a) shows that the network lifetime decreases and the utility increases as the increment of α. On the contrary, we can observe that as the weighted system parameter α decreases, the corresponding optimal network lifetime increases. It can be seen in Fig. 9(b) that the lifetime increases to 8.5s from 4.5s. Fig. 10(a) shows the harvested energy profile from (16) for the farthest node in the network. Replacing the optimal s_{ij}^*, R_{ij}^* in (30), $P_{H_i}^C(t)$ is found using $f^{-1}\left(g(s_{ij}^*, R_{ij}^*)\right)$ as shown in Fig. 10(b). Further, if wake-up radio scheme is applied with energy harvesting, the lifetime increases to ∼10s as in Fig. 9(c). The network utility of the system also increases to 0.87 with energy harvesting and 0.97 with both energy harvesting and WUR. Hence, based on the desired performance of the system, designer can chose the value of α and solve the set of equations for optimal lifetime and source node rates.

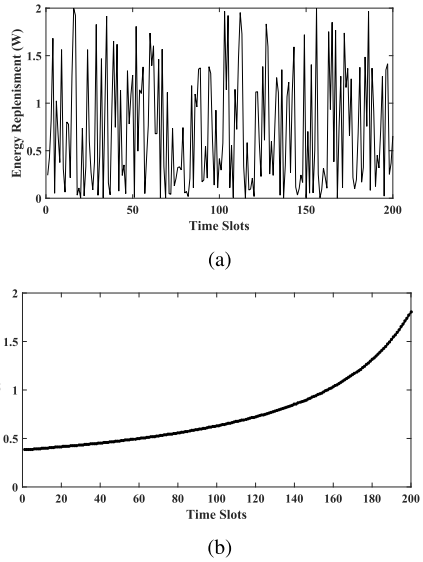

FIGURE 10. Energy harvesting profile and allocated energy plots. (a) Replenishment profile for harvested energy. (b) Energy resource allocation.

C. IMPACT OF ERROR CONTROL CODING ON PERFORMANCE AND LIFETIME

Fig. 9(d) shows the utility-lifetime trade-off with error coding applied. The system lifetime is further increased as compared to Fig. 9(a)-(c), to 14s and the network is more utilized at 91%. To visualize the impact of error coding on the performance of the system, we plot the network lifetime versus the packet loss rate P_e^i at $\alpha = 0.1$. Fig. 11(a) shows the plot of network lifetime for different cases with packet loss rate varying from 0 to 20%. For a packet loss rate between 10% to 20%, the network lifetime increases more than 3 times with only energy harvesting and wake-up radio scheme. Whereas with the coding scheme applied, it doubles further giving a 6 times improvement. We evaluate the network lifetime of nodes $\{i1, i3, i5, i6\}$, where $\{i1, i5\}$ act as only sensor nodes and $\{i3, i6\}$ act as both sensor and relay node. The network lifetime is shown in Fig. 11(b) versus the system parameter α incorporating harvesting and coding at packet loss rate

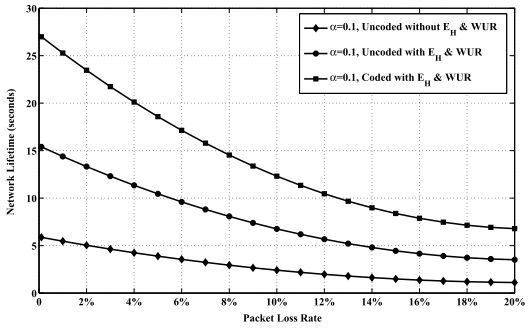

(a)

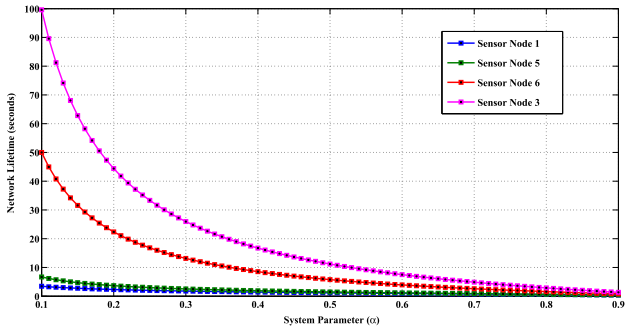

(b)

FIGURE 11. Impact of ECC on lifetime of sensor nodes. (a) Plot of network lifetime versus packet loss rate. (b) Network lifetime of different sensor nodes versus system parameter α.

of 20%. As expected from (23), the lifetime of node $i1$ is the least. Relaying of data from $i5 \rightarrow i6$ improves the lifetime of node $i5$. Nodes $i3$ and $i6$ have a huge improvement in their lifetime owing to their proximity to the sink node from where they harvest energy according to (15). Even though the total energy consumption is increased, the harvested energy increase is sufficient enough to boost its lifetime.

D. EFFECT OF ENERGY HARVESTING AND ERROR CORRECTING CODES ON PRACTICAL SENSOR NODE TelosB

For analyzing the effect of our error correcting codes performance on node lifetime, we have taken real time sensor energy cost from [40] for different sensors as shown in Table 4. The Table shows different commonly used sensing devices, their E_{PR} and E_{SN} energy cost normalized w.r.t communication energy E_{comm} for common sensor mote **TelosB** (TelosB is a IEEE 802.15.4 compliant sensor mote that runs a TinyOS operating system with a CC2420 radio. http://www.willow.co.uk/TelosB_Datasheet.pdf).

Where, E_{comm} is sum of E_{TX} and E_{RX}. Using different energy cost of sensors from Table 4, we have plotted curve for **TelosB** mote. The battery power is taken as 9000 milli-Amphere-Hour (capacity of 2 standard $1.5 - volt$ batteries used in sensors). Fig. 12(a) is drawn for RRNS, BCH, and ARQ for a packet loss rate of 20% showing the estimated lifetime in days for the **TelosB** mote versus the total

TABLE 4. Processing and sensing energy cost of sensing devices for TelosB mote w.r.t $E_{comm} = 1mW$.

	TelosB Mote	
Sensors Type & Model No.	$\frac{E_{PR}}{E_{comm}}$	$\frac{E_{SN}}{E_{comm}}$
Acceleration MMA72600Q	0.044	0.000027
Pressure 2200/2600 Series	0.044	0.00013
Light ISL 29002 18	0.047	0.00068
Proximity CP 18	0.047	0.267
Humidity SHT 1X	0.043	0.4
Temperature SHT 1X	0.94	1.5

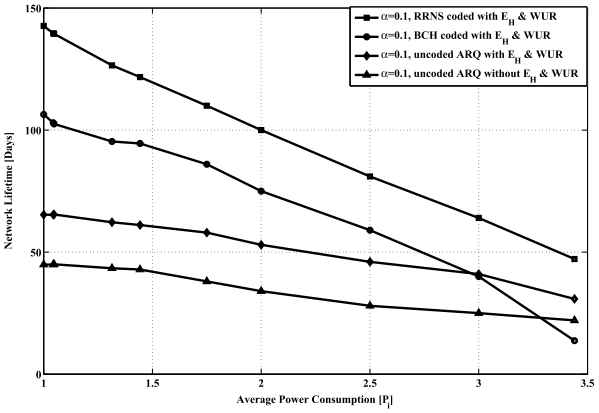

(a)

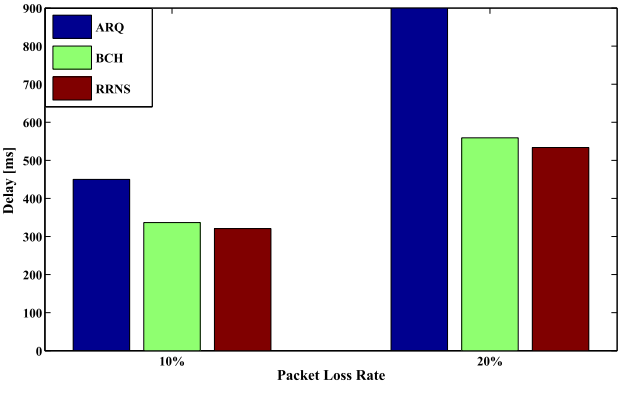

(b)

FIGURE 12. Impact of WEH & ECC on TelosB mote. (a) Network Lifetime prediction of ARQ, BCH, and RRNS schemes. (b) Transmission Delay performance of ARQ, BCH, and RRNS schemes.

average power consumption P_i from (11). For low power sensors i.e *acceleration*, *pressure*, *light*, *proximity* given in Table 4, TelosB motes lifetime increases by $\sim$1.7 times

with BCH error scheme and more than ***doubles*** with RRNS error scheme. Whereas for power hungry sensor such as *Temperature*, the processing energy is higher, thus overpowering the effect of small number of retransmissions in error coding schemes.

One of the major overheads of error correcting codes in addition to transmission and reception of redundant bits is the delay associated with encoding and decoding of packets. Let us assume that t^{ARQ} is the total time required for sending the packets to the sink node and receiving an *ACK* back. Further, if the decoding latency of a block code like (n, k, e) BCH is t_{dec}^{BCH}. From [24], the decoding latency is given by

$$t_{dec}^{BCH} = (2ne + 2e^2)(t_{add} + t_{mult})\left\lceil \frac{b}{b_m} \right\rceil \tag{34}$$

Here, t_{add} and t_{mult} are time required for additions and multiplications in GF (2^b), and b_m is the number of bits of micro controller used in sensor nodes. In an 8-bit micro controller, t_{add} take one cycle and t_{mult} takes two cycles as computation time. The number of cycles depends on the frequency of the micro controller.

RRNS codes of form $((2^{b-1} - 1, 2^{b-1}; 2^{b-1} + 1, 2^b + 1))$ needs $\frac{t^{ARQ}}{(k/n)}$ as the total time required for sending the packets to the sink node and receiving *ACK* back. The decoding latency depends on the total additions and multiplications in the number of iterations $\binom{\delta}{\beta}$. Depending on the value of β for each step there are 2β multiplications and β additions involved. Further, there are $\binom{\delta}{\beta}$ number of moduli operations involved. Thus, the decoding latency for RRNS codes is

$$t_{dec}^{RRNS} = \left(\binom{\delta}{\beta} t_{add} + \binom{\delta}{\beta} t_{mult}\right)\left\lceil \frac{b}{b_m} \right\rceil + \left(\binom{\delta}{\beta} e\right)\left\lceil \frac{e}{b_m} \right\rceil \tag{35}$$

To analyze the effectiveness of the coding schemes, we have plotted the delay in sending one packet of data versus the packet loss rate of 10% and 20%. If we take $t^{ARQ} = 50ms$, from (34) and (35), delays of BCH(127, 57, 11) and RRNS(128, 60, 32) can be found as $t_{delay}^{BCH} = t^{ARQ} * (n/k) + t_{dec}^{BCH}$ and $t_{delay}^{RRNS} = t^{ARQ} * (n/k) + t_{dec}^{RRNS}$. **TelosB** has a 16-bit microcontroller and its clock frequency is 8MHZ. Fig. 12(b) shows the delay in milliseconds. It can be inferred that the coding schemes outperforms the ARQ sheme in terms of total transmission delay. RRNS scheme has less delay compared to BCH coding due to its better coding rate and faster decoding. It can also be seen that as the packet loss rate increases, the delay gap between the three schemes increases. Thus RRNS has better performance in terms of lifetime improvement as well as lower delay as the packet loss rate increases in bad channel conditions.

E. GREEN NETWORKING: REDUCTION IN CARBON FOOTPRINT

For network to be green, the carbon emissions has to be reduced. The index of measure of carbon emissions is Xgr of CO_2 per year. For each packet loss in the network causes the data server station or the sink node to transmit back *NACK* to sensor node. The transmitting power (P_{TX}^S) of the data station depends on the fuel type from which the station derives its electrical power. Depending on the country, it can be coal or gas. Thus value of X can be either 870 or 370 [20]. (P_{TX}^S) depends on the type of technology used. If we assume that the sink node data station runs on the Long Term Evolution (LTE) network and uses the static micro cell topology with radius 100m. Then from [41] and [20], the carbon footprint generated by sink node is

$$F_{CO_2}^S = P_{TX}^S \cdot (E_{T,h_i} + 1) \cdot 8.64 \cdot 10^{-3} \cdot X[KgCO_2/Year]$$
$$P_{TX}^S = \left(\frac{P_{TX}^D}{\mu_{PA}} C_{TX,static} + P_{SP,static}\right)(1 + C_{PS}) \tag{36}$$

TABLE 5. LTE micro base station based sink node power model parameters.

Parameter	Description	Value
P_{TX}^D	Power consumed by sink node base station server	2 W
μ_{PA}	Power Amplifier efficiency	20%
$C_{TX,static}$	Static transmitted power	0.8
$P_{SP,static}$	Static signal processing power	15 W
C_{PS}	Power supply loss	0.11

Where, the notations are described in Table 5. Apart from the sink node, the battery is also responsible for generation of carbon footprint. Typical AA batteries used in sensors have a end of life carbon emission of 4.3 $KgCO_2$ per 30 batteries [42]. Thus, the carbon footprint $[KgCO_2/Year]$ generated by number of batteries used is directly proportional to the total batteries used in a year (B_u^{year}) and is given as

$$F_{CO_2}^B = B_u^{year}\left(\frac{4.3}{30}\right)[KgCO_2/Year], \quad B_u^{year} = \frac{365}{T_{network}} \tag{37}$$

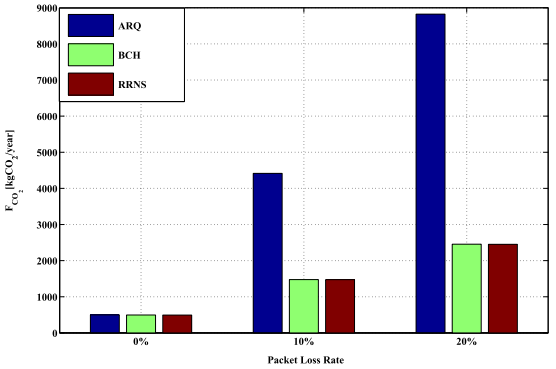

FIGURE 13. Plot of packet loss rate versus carbon footprint.

The total carbon footprint (F_{CO_2}) is therefore the sum of carbon footprints in (36) and (37). To show the effectiveness of using ECC, WEH & WUR, we plot F_{CO_2} for different

packet loss rate of (0, 10, 20). We take X=370, the fuel for production of electricity as gas. The $T_{network}$ for different schemes ARQ, RRNS and BCH are taken from Fig. 12(a) at $P_i = 1$mW. Fig. 13 shows the carbon footprint at different schemes. It can be seen that as the packet loss rate increases, the carbon footprint is tremendously reduced for RRNS and BCH. It is ∼2.5 times lesser kgCO_2 per year at 10% packet loss and ∼4 times lesser kgCO_2 per year at 20% packet loss. So, as the channel goes bad, the carbon emissions for normal scheme like ARQ increases tremendously, whereas incorporation ECC and harvesting the network becomes more greener.

VIII. CONCLUSION

Enabling technologies and schemes to facilitate green wireless sensor networks are presented. Wireless energy harvesting is investigated as a remedy to prolong the lifetime of sensor nodes and enable maintenance-free operation. Wake-up radio scheme is incorporated as an efficient solution to address the idle listening energy dissipation of sensor nodes. RRNS Error control coding is proposed to improve the reliability of the transmission and reduce re-transmission, hence, reducing energy consumption. A utility-lifetime maximization problem incorporating WEH, WUR and ECC schemes is formulated and solved using distributed dual subgradient algorithm based on Lagrange multiplier method. Simulation results verify the effectiveness of the proposed schemes in reducing the energy consumption and accordingly, carbon footprint of wireless sensor nodes, providing the means for a greener wireless sensor network.

APPENDIX A
PROOF OF LEMMA 2

We define $\bar{E}^1$ and $\bar{E}^2$ in $\Re^{|N|+|L(i)|}$ as $E_{TX}(1 + E(T, h_i)) + E_{RX}(1 + E(T, h_i))$ and $E_{PR}(1 + E(T, h_i)P^{'}) + R_{ij}E_{SN}$ respectively. If we denote ∞-norm as $\|.\|_\infty$ and q-norm as $\|.\|_q$, the lifetime objective functions of (14) and (24) are represented by -$\|\bar{E}^1 r + \bar{E}^2 R\|_\infty$ and -$(1/(\epsilon+1))\|\bar{E}^1 r + \bar{E}^2 R\|_{\epsilon+1}$ respectively. Suppose $\{r^*, R^*\}$ and $\{r^*_\epsilon, R^*_\epsilon\}$ be the optimal solutions for the two objective functions. Then we have the following inequalities using approximation of $\|.\|_\infty$ from [43]

$$\begin{aligned}
&\|\bar{E}^1 r^*_\epsilon + \bar{E}^2 R^*_\epsilon\|_\infty \\
&\quad \le \|\bar{E}^1 r^*_\epsilon + \bar{E}^2 R^*_\epsilon\|_{\epsilon+1} \\
&\quad \le \|\bar{E}^1 r^* + \bar{E}^2 R^*\|_{\epsilon+1} \\
&\quad \le |N|^{1/(\epsilon+1)}\|\bar{E}^1 r^* + \bar{E}^2 R^*\|_\infty
\end{aligned} \tag{38}$$

The corresponding network lifetimes become T_i=$1/\|\bar{E}^1 r^* + \bar{E}^2 R^*\|_\infty$ and T^ϵ_i=$1/\|\bar{E}^1 r^*_\epsilon + \bar{E}^2 R^*_\epsilon\|_\infty$. From (39) we have,

$$\frac{1}{|N|^{1/(\epsilon+1)}} T_i \le T^\epsilon_i \le T_i \tag{39}$$

At $lim_{\epsilon\to\infty} T^\epsilon_i = T_i$, and thus the lemma holds.

APPENDIX B
PROOF OF PROPOSITION 2

From (27), the gradient of the objective function od $D(\lambda, \mu)$ w.r.t λ_l,

$$\begin{aligned}
\nabla_\lambda D(\lambda, \mu) &= \alpha \sum_{i\in N}\sum_{j\in N_i} \nabla_\lambda U_i(R_{ij}, P_s) - (1-\alpha) s^\epsilon_i \cdot \nabla_\lambda s_i \\
&\le \alpha \sum_{i\in N}\sum_{j\in N_i} \nabla_\lambda U_i(R_{ij}, P_s) \le \alpha \overline{U}
\end{aligned} \tag{40}$$

By **Definition 1** and **Assumption 1**, we can find the error in the cost estimation of the link price λ_l when iteration $c \to c+1$

$$\begin{aligned}
\|D(\lambda(c+1)) - D(\lambda(c))\| &\le \|\nabla_\lambda D(\lambda)^T(\lambda(c+1) - \lambda(c))\| \\
&\le \|\nabla_\lambda D(\lambda)\| \cdot \|(\lambda(c+1) - \lambda(c))\| \\
&\le \overline{L}^{1/2} \alpha \overline{U} \|(\lambda(c+1) - \lambda(c))\|
\end{aligned} \tag{41}$$

From the above inequalities, we see that function is Lipschitz. Thus the solution generated with step size φ_c is optimal [43]. Let the update at each iteration c is given by $\Delta\lambda(c)$. Then,

$$\begin{aligned}
|\Delta(\lambda(c))| &= \left|\frac{r_{ij}(c)}{\alpha \nabla_\lambda U_i(R_{ij}, P_s)} \nabla_\lambda D(\lambda)\right| \\
&\le \frac{\overline{R}}{\alpha} |\nabla_\lambda D(\lambda)|
\end{aligned} \tag{42}$$

$$\frac{|\nabla_\lambda D(\lambda)^T \Delta(\lambda(c))|}{\|\Delta(\lambda(c))\|^2} \le \frac{\frac{\overline{R}}{\alpha}\|\nabla_\lambda D(\lambda)\|^2}{(\frac{\overline{R}}{\alpha})^2 \|\nabla_\lambda D(\lambda)\|^2} = \frac{\alpha}{\overline{R}} \tag{43}$$

According to [43], the step size satisfies $0 < \varphi_c < \frac{2}{\overline{L}^{1/2}\overline{U}\,\overline{R}}$. Similarly, the step size bound can be proven for ψ_c.

REFERENCES

[1] N. A. Pantazis, S. A. Nikolidakis, and D. D. Vergados, "Energy-efficient routing protocols in wireless sensor networks: A survey," *IEEE Commun. Surveys Tut.*, vol. 15, no. 2, pp. 551–591, 2nd Quart. 2013.

[2] M. Webb. (2008). *SMART 2020: Enabling the Low Carbon Economy in the Information Age, A Report by The Climate Group on Behalf of the Global eSustainability Initiative (GeSI)*. [Online]. Available: http://www.smart2020.org/publications/

[3] F. P. Kelly, A. K. Maulloo, and D. K. Tan, "Rate control for communication networks: Shadow prices, proportional fairness and stability," *J. Oper. Res. Soc.*, vol. 49, no. 3, pp. 237–252, 1998.

[4] R. Madan and S. Lall, "Distributed algorithms for maximum lifetime routing in wireless sensor networks," *IEEE Trans. Wireless Commun.*, vol. 5, no. 8, pp. 2185–2193, Aug. 2006.

[5] S. Ehsan, B. Hamdaoui, and M. Guizani, "Radio and medium access contention aware routing for lifetime maximization in multichannel sensor networks," *IEEE Trans. Wireless Commun.*, vol. 11, no. 9, pp. 3058–3067, Sep. 2012.

[6] J. Chen, W. Xu, S. He, Y. Sun, P. Thulasiraman, and X. Shen, "Utility-based asynchronous flow control algorithm for wireless sensor networks," *IEEE J. Sel. Areas Commun.*, vol. 28, no. 7, pp. 1116–1126, Sep. 2010.

[7] S. He, J. Chen, D. K. Y. Yau, and Y. Sun, "Cross-layer optimization of correlated data gathering in wireless sensor networks," in *Proc. 7th Annu. IEEE Commun. Soc. Conf. Sensor Mesh Ad Hoc Commun. Netw. (SECON)*, Jun. 2010, pp. 1–9.

[8] D. S. Lun, M. Médard, R. Koetter, and M. Effros, "On coding for reliable communication over packet networks," *Phys. Commun.*, vol. 1, no. 1, pp. 3–20, 2008.

[9] K. Yu, F. Barac, M. Gidlund, and J. Åkerberg, "Adaptive forward error correction for best effort wireless sensor networks," in *Proc. IEEE Int. Conf. Commun. (ICC)*, Jun. 2012, pp. 7104–7109.
[10] W. Xu, Q. Shi, X. Wei, Z. Ma, X. Zhu, and Y. Wang, "Distributed optimal rate–reliability–lifetime tradeoff in time-varying wireless sensor networks," *IEEE Trans. Wireless Commun.*, vol. 13, no. 9, pp. 4836–4847, Sep. 2014.
[11] J. Zou, H. Xiong, C. Li, R. Zhang, and Z. He, "Lifetime and distortion optimization with joint source/channel rate adaptation and network coding-based error control in wireless video sensor networks," *IEEE Trans. Veh. Technol.*, vol. 60, no. 3, pp. 1182–1194, Mar. 2011.
[12] T. He, K.-W. Chin, and S. Soh, "On wireless power transfer and max flow in rechargeable wireless sensor networks," *IEEE Access*, vol. 4, pp. 4155–4167, Aug. 2016.
[13] M. Magno, D. Boyle, D. Brunelli, E. Popovici, and L. Benini, "Ensuring survivability of resource-intensive sensor networks through ultra-low power overlays," *IEEE Trans. Ind. Informat.*, vol. 10, no. 2, pp. 946–956, May 2014.
[14] R. Deng, Y. Zhang, S. He, J. Chen, and X. S. Shen, "Globally optimizing network utility with spatiotemporally-coupled constraint in rechargeable sensor networks," in *Proc. IEEE Global Commun. Conf. (GLOBECOM)*, Dec. 2013, pp. 4810–4815.
[15] P. Kamalinejad, C. Mahapatra, Z. Sheng, S. Mirabbasi, V. C. M. Leung, and Y. L. Guan, "Wireless energy harvesting for the Internet of things," *IEEE Commun. Mag.*, vol. 53, no. 6, pp. 102–108, Jun. 2015.
[16] J. M. Gilbert and F. Balouchi, "Comparison of energy harvesting systems for wireless sensor networks," *Int. J. Autom. Comput.*, vol. 5, no. 4, pp. 334–347, Oct. 2008.
[17] Z. Mao, C. E. Koksal, and N. B. Shroff, "Near optimal power and rate control of multi-hop sensor networks with energy replenishment: Basic limitations with finite energy and data storage," *IEEE Trans. Autom. Control*, vol. 57, no. 4, pp. 815–829, Apr. 2012.
[18] S. Chen, P. Sinha, N. B. Shroff, and C. Joo, "Finite-horizon energy allocation and routing scheme in rechargeable sensor networks," in *Proc. IEEE INFOCOM*, Apr. 2011, pp. 2273–2281.
[19] A. Biason and M. Zorzi, "Joint online transmission and energy transfer policies for energy harvesting devices with finite batteries," in *Proc. 21th Eur. Wireless Conf., Eur. Wireless*, 2015, pp. 1–7.
[20] G. Koutitas, "Green network planning of single frequency networks," *IEEE Trans. Broadcast.*, vol. 56, no. 4, pp. 541–550, Dec. 2010.
[21] M. Naeem, U. Pareek, D. C. Lee, and A. Anpalagan, "Estimation of distribution algorithm for resource allocation in green cooperative cognitive radio sensor networks," *Sensors*, vol. 13, no. 4, pp. 4884–4905, 2013.
[22] S. Boyd and L. Vandenberghe, *Convex Optimization*. Cambridge, U.K.: Cambridge Univ. Press, 2004.
[23] C. Mahapatra, Z. Sheng, V. Leung, and T. Stouraitis, "A reliable and energy efficient iot data transmission scheme for smart cities based on redundant residue based error correction coding," in *Proc. 12th Annu. IEEE Int. Conf. Sens., Commun., Netw.-Workshops (SECON Workshops)*, Jun. 2015, pp. 1–6.
[24] M. C. Vuran and I. F. Akyildiz, "Error control in wireless sensor networks: A cross layer analysis," *IEEE/ACM Trans. Netw.*, vol. 17, no. 4, pp. 1186–1199, Aug. 2009.
[25] J.-D. Sun and H. Krishna, "A coding theory approach to error control in redundant residue number systems. II. Multiple error detection and correction," *IEEE Trans. Circuits Syst. II, Analog Digit. Signal Process.*, vol. 39, no. 1, pp. 18–34, Jan. 1992.
[26] W. Jenkins and E. J. Altman, "Self-checking properties of residue number error checkers based on mixed radix conversion," *IEEE Trans. Circuits Syst.*, vol. 35, no. 2, pp. 159–167, Feb. 1988.
[27] X. Lu, P. Wang, D. Niyato, D. I. Kim, and Z. Han, "Wireless networks with RF energy harvesting: A contemporary survey," *IEEE Commun. Surveys Tut.*, vol. 17, no. 2, pp. 757–789, 2014. [Online]. Available: http://arxiv.org/abs/1406.6470
[28] K. Xie, Y.-M. Liu, H.-L. Zhang, and L.-Z. Fu, "Harvest the ambient AM broadcast radio energy for wireless sensors," *J. Electromagn. Waves Appl.*, vol. 25, nos. 14–15, pp. 2054–2065, 2011. [Online]. Available: http://dx.doi.org/10.1163/156939311798072144
[29] M. Russo, P. Šolić, and M. Stella, "Probabilistic modeling of harvested GSM energy and its application in extending UHF RFID tags reading range," *J. Electromagn. Waves Appl.*, vol. 27, no. 4, pp. 473–484, 2013. [Online]. Available: http://dx.doi.org/10.1080/09205071.2013.753659
[30] S. He, J. Chen, F. Jiang, D. K. Y. Yau, G. Xing, and Y. Sun, "Energy provisioning in wireless rechargeable sensor networks," *IEEE Trans. Mobile Comput.*, vol. 12, no. 10, pp. 1931–1942, Oct. 2013.
[31] P. Kamalinejad, K. Keikhosravy, R. Molavi, S. Mirabbasi, and V. C. M. Leung, "Efficiency enhancement techniques and a dual-band approach in RF rectifiers for wireless power harvesting," in *Proc. IEEE Int. Symp. Circuits Syst. (ISCAS)*, Jun. 2014, pp. 2049–2052.
[32] V. Jelicic, M. Magno, D. Brunelli, V. Bilas, and L. Benini, "Analytic comparison of wake-up receivers for WSNs and benefits over the wake-on radio scheme," in *Proc. 7th ACM Workshop Perform. Monitor. Meas. Heterogeneous Wireless Wired Netw.*, New York, NY, USA, 2012, pp. 99–106. [Online]. Available: http://doi.acm.org/10.1145/2387191.2387206
[33] V. Jelicic, M. Magno, D. Brunelli, V. Bilas, and L. Benini, "Benefits of wake-up radio in energy-efficient multimodal surveillance wireless sensor network," *IEEE Sensors J.*, vol. 14, no. 9, pp. 3210–3220, Sep. 2014.
[34] P. Kamalinejad, K. Keikhosravy, M. Magno, S. Mirabbasi, V. C. M. Leung, and L. Benini, "A high-sensitivity fully passive wake-up radio front-end for wireless sensor nodes," in *Proc. IEEE Int. Conf. Consumer Electron. (ICCE)*, Jan. 2014, pp. 209–210.
[35] P. Huang, L. Xiao, S. Soltani, M. W. Mutka, and N. Xi, "The evolution of MAC protocols in wireless sensor networks: A survey," *IEEE Commun. Surveys Tut.*, vol. 15, no. 1, pp. 101–120, 1st Quart. 2013.
[36] A. N. Alvi, S. H. Bouk, S. H. Ahmed, M. A. Yaqub, N. Javaid, and D. Kim, "Enhanced TDMA based MAC protocol for adaptive data control in wireless sensor networks," *J. Commun. Netw.*, vol. 17, no. 3, pp. 247–255, Jun. 2015.
[37] S. Kosunalp, "A new energy prediction algorithm for energy-harvesting wireless sensor networks with q-learning," *IEEE Access*, vol. 4, pp. 5755–5763, Sep. 2016.
[38] A. N. Alvi, S. H. Bouk, S. H. Ahmed, M. A. Yaqub, M. Sarkar, and H. Song, "Best-mac: Bitmap-assisted efficient and scalable tdma-based wsn mac protocol for smart cities," *IEEE Access*, vol. 4, pp. 312–322, 2016.
[39] M. Bhardwaj and A. Chandrakasan, "Bounding the lifetime of sensor networks via optimal role assignments," in *Proc. IEEE 21st Annu. Joint Conf. IEEE Comput. Commun. Soc. (INFOCOM)*, vol. 3. Jun. 2002, pp. 1587–1596.
[40] M. A. Razzaque and S. Dobson, "Energy-efficient sensing in wireless sensor networks using compressed sensing," *Sensors*, vol. 14, no. 2, pp. 2822–2859, 2014.
[41] O. Arnold, F. Richter, G. Fettweis, and O. Blume, "Power consumption modeling of different base station types in heterogeneous cellular networks," in *Proc. Future Netw. Mobile Summit*, Jun. 2010, pp. 1–8.
[42] E. Olivetti, J. Gregory, and R. Kirchain, "Life cycle impacts of alkaline batteries with a focus on end-of-life," in *Proc. Study Conducted Nat. Electr. Manuf. Assoc.*, 2011, pp. 1–108
[43] D. Bertsekas, *Nonlinear Programming*. Belmont, MA, USA: Athena Scientific, 1995. [Online]. Available: http://books.google.ca/books?id=QeweAQAAIAAJ

CHINMAYA MAHAPATRA received the B.Tech. degree in electronics and communication engineering from the National Institute of Technology, Rourkela, India, in 2009, and the M.A.Sc. degree in electrical and computer engineering from The University of British Columbia (UBC), Vancouver, BC, Canada in 2013, where he is currently pursuing the Ph.D. degree with the Department of Electrical and Computer Engineering.

He was a Scientist with the Indian Defense Research Laboratory, and a Systems Engineer with the Ciena Research and Development Center, Ottawa, Canada. His interests include the Internet of Things, body sensor area networks, embedded systems, sensor cloud, and energy optimization. He currently holds the Doctoral scholarship awarded by NSERC and four-year fellowship by UBC.

ZHENGGUO SHENG received the B.Sc. degree from the University of Electronic Science and Technology of China in 2006, and the M.S. and Ph.D. degrees (Hons.) from the Imperial College London in 2011 and 2007, respectively.

He was with UBC as a Research Associate and with France Telecom Orange Labs as a Senior Researcher and a Project Manager in M2M/IoT. He is currently a Lecturer with the School of Engineering and Informatics, University of Sussex, U.K. He was a Research Intern with IBM T. J. Watson Research Center, USA, and U.S. Army Research Labs. He has authored over 60 international conference and journal papers.

POUYA KAMALINEJAD received the B.Sc. and M.Sc. degrees in electrical and computer engineering from the University of Tehran, Iran, in 2006 and 2008, respectively, and the Ph.D. degree in electrical and computer engineering from The University of British Columbia, Canada, in 2014.

He is a Post-Doctoral Fellow with the University of British Columbia. His current interests include RF and low-power integrated circuit design, wireless energy harvesting for RFID tags and wireless sensor networks, sensors, and sensor interface design.

VICTOR C.M. LEUNG (S'75–M'89–SM'97–F'03) received the B.A.Sc. degree (Hons.) in electrical engineering from The University of British Columbia (UBC) in 1977, and the Ph.D. degree in electrical engineering in 1981. He received the APEBC Gold Medal as the head of the graduating class in the Faculty of Applied Science. He attended graduate school at UBC on a Natural Sciences and Engineering Research Council Postgraduate Scholarship.

From 1981 to 1987, he was a Senior Member of the Technical Staff and Satellite System Specialist with MPR Teltech Ltd., Canada. In 1988, he was a Lecturer with the Department of Electronics, Chinese University of Hong Kong. He returned to UBC as a Faculty Member in 1989, where he is currently a Professor and a TELUS Mobility Research Chair in Advanced Telecommunications Engineering with the Department of Electrical and Computer Engineering. He has co-authored over 700 technical papers in international journals and conference proceedings, 29 book chapters, and co-edited eight book titles. His research interests are in the areas of wireless networks and mobile systems. Several of his papers had been selected for Best Paper awards.

Dr. Leung is a Registered Professional Engineer in the Province of British Columbia, Canada. He is a fellow of the Royal Society of Canada, the Engineering Institute of Canada, and the Canadian Academy of Engineering. He received the IEEE Vancouver Section Centennial Award and the 2012 UBC Killam Research Prize. He was a Distinguished Lecturer of the IEEE Communications Society. He is a member of the Editorial Boards of the IEEE Wireless Communications Letters, *Computer Communications*, and several other journals. He has served on the Editorial Boards of the IEEE Journal on Selected Areas in Communications Wireless Communications Series, the IEEE Transactions on Wireless Communications, the IEEE Transactions on Vehicular Technology, the IEEE Transactions on Computers, and the *Journal of Communications and Networks*. He has guest-edited many journal special issues, and contributed to the organizing committees and technical program committees of numerous conferences and workshops.

SHAHRIAR MIRABBASI received the B.Sc. degree in electrical engineering from Sharif University of Technology, Tehran, Iran, in 1990, and the M.A.Sc. and Ph.D. degrees in electrical and computer engineering from the University of Toronto, Ontario, Canada, in 1997 and 2002, respectively.

Since 2002, he has been with the Department of Electrical and Computer Engineering, The University of British Columbia, Canada, where he is currently a Professor. His research interests include analog, mixed-signal, RF, and mmWave integrated circuit and system design, with particular emphasis on communication, sensor interface, and biomedical applications.